

Functional analysis of *Saccharomyces cerevisiae* FLO genes through optogenetic control

Ignacia, Denzel G.L.; Bennis, Nicole X.; Wheeler, Caitlyn; Tu, Lylyna C.L.; Keijzer, Jelle; Cardoso, Clara Carqueija; Daran, Jean Marc G.

DOI

[10.1093/femsyr/foaf057](https://doi.org/10.1093/femsyr/foaf057)

Publication date

2025

Document Version

Final published version

Published in

FEMS yeast research

Citation (APA)

Ignacia, D. G. L., Bennis, N. X., Wheeler, C., Tu, L. C. L., Keijzer, J., Cardoso, C. C., & Daran, J. M. G. (2025). Functional analysis of *Saccharomyces cerevisiae* FLO genes through optogenetic control. *FEMS yeast research*, 25, Article foaf057. <https://doi.org/10.1093/femsyr/foaf057>

Important note

To cite this publication, please use the final published version (if applicable).
Please check the document version above.




Copyright

Other than for strictly personal use, it is not permitted to download, forward or distribute the text or part of it, without the consent of the author(s) and/or copyright holder(s), unless the work is under an open content license such as Creative Commons.

Takedown policy

Please contact us and provide details if you believe this document breaches copyrights.
We will remove access to the work immediately and investigate your claim.

Functional analysis of *Saccharomyces cerevisiae* FLO genes through optogenetic control

Denzel G. L. Ignacia , Nicole X. Bennis , Caitlyn Wheeler, Lylyna C. L. Tu, Jelle Keijzer, Clara Carqueija Cardoso, Jean-Marc G. Daran 

Department of Biotechnology, Delft University of Technology, van der Maasweg 9, 2629HZ Delft, The Netherlands

*Corresponding author. Department of Biotechnology, Delft University of Technology, van der Maasweg 9, 2629HZ Delft, The Netherlands. E-mail: J.g.Daran@tudelft.nl

Editor: Isak Pretorius

Abstract

Flocculation in *Saccharomyces cerevisiae* is a critical phenotype with ecological and industrial significance. This study aimed to functionally dissect the contributions of individual FLO genes (FLO1, FLO5, FLO9, FLO10, FLO11) to flocculation by employing an optogenetic circuit (OptoQ-AMP5) for precise, light-inducible control of gene expression. A FLO-null platform yeast strain was engineered allowing the expression of individual FLO genes without native background interference. Each FLO gene was reintroduced into the FLO-null background under the control of OptoQ-AMP5. Upon light induction, strains expressing FLO1, FLO5, or FLO10 demonstrated strong flocculation, with FLO1 and FLO5 forming large and structurally distinct aggregates. FLO9 induced a weaker phenotype. Sugar inhibition assays revealed distinct sensitivities among flocculins, notably FLO9's novel sensitivity to fructose and maltotriose. Additionally, FLO-induced changes in cell surface hydrophobicity were quantified, revealing that FLO10 and FLO1 conferred the greatest hydrophobicity, correlating with their aggregation strength. This work establishes a robust platform for investigating flocculation mechanisms in yeast with temporal precision. It highlights the phenotypic diversity encoded within the FLO gene family and their differential responses to environmental cues. The optogenetic system provides a valuable tool for both fundamental studies and the rational engineering of yeast strains for industrial fermentation processes requiring controlled flocculation.

Keywords: optogenetics; flocculation; gene expression; *Saccharomyces cerevisiae*

Introduction

Microbial aggregation is fundamental for cell survival and communication in the natural environment (Goossens et al. 2015), providing protection against stresses and facilitating resource sharing (Verstrepen et al. 2004). In yeasts, flocculation, a reversible, calcium-dependent, asexual aggregation, has emerged as a critical phenomenon. It enables yeast to form multi cellular aggregates or “flocs” (Burns 1937), which shield cells from temperature and pH fluctuations, and enhance survival under nutrient-limitation through nutrient release from lysed cells at the floc's core (Verstrepen et al. 2004). Beyond its ecological significance, flocculation has major industrial relevance, particularly in the beer, wine, and bioethanol production, where it allows cost-effective biomass separation (Stratford 1996, Sampermans et al. 2005, Vallejo et al. 2013). In lager brewing, timing is crucial, as premature flocculation leads to incomplete fermentation and undesirable flavour profiles (Panteloglou et al. 2012, He et al. 2022), while delayed flocculation hampers cell recovery and clarity (Stewart 2018).

In *Saccharomyces cerevisiae*, flocculation is mainly mediated by the FLO gene family, which encodes cell-surface adhesins forming lectin-like bonds with mannose residues of α -mannan polysaccharides of glycosylated proteins in cell wall of neighbouring cells in the presence of Ca^{2+} (Miki et al. 1982). Some flocculins also

contribute to cell-substrate adhesion and biofilm formation (Verstrepen and Klis 2006). Brewing relevant FLO genes fall into two subgroups: i) FLO1, FLO5, FLO9 and FLO10 for cell-cell adhesion (Theunissen and Steensma 1995) and ii) FLO11 for pseudohyphal invasive growth and cell-substrate adhesion (Lambrechts et al. 1996, Guo et al. 2000).

Flocculins share three domains (Figure 1): a N-terminal mannose-binding domain (PA14 carbohydrate binding domain family), a central serine–threonine-rich tandem repeats region (Verstrepen et al. 2004, Veelders et al. 2010) and a C-terminal glycosylphosphatidylinositol (GPI)-anchor linking the protein to the cell wall (Der Vaart et al. 1996, Caro et al. 1997). The subtelomeric localization of the FLO genes promote recombination and replication slippage, resulting in phenotypic variability across yeast strains (Smukalla et al. 2008). Two major flocculation phenotypes exist: Flo1 inhibited mainly by mannose, and NewFlo, common in brewing strains and inhibited by several sugars including mannose, maltose, glucose and sucrose (Stratford and Assinder 1991, Liu et al. 2007). Wort used in beer brewing contains maltose, maltotriose, and glucose, along with smaller amounts of fructose and sucrose (Stewart 2016), which can inhibit flocculation by competing with flocculins. Variations in the repeat regions of flocculins (Figure 1) affects floc size, sedimentation rates, and sugar inhibition profiles, further complicating the regulation of this pheno-

Received 14 July 2025; revised 5 September 2025; accepted 22 September 2025

© The Author(s) 2025. Published by Oxford University Press on behalf of FEMS. This is an Open Access article distributed under the terms of the Creative Commons Attribution-NonCommercial-NoDerivs licence (<https://creativecommons.org/licenses/by-nc-nd/4.0/>), which permits non-commercial reproduction and distribution of the work, in any medium, provided the original work is not altered or transformed in any way, and that the work is properly cited. For commercial re-use, please contact reprints@oup.com for reprints and translation rights for reprints. All other permissions can be obtained through our RightsLink service via the Permissions link on the article page on our site-for further information please contact journals.permissions@oup.com

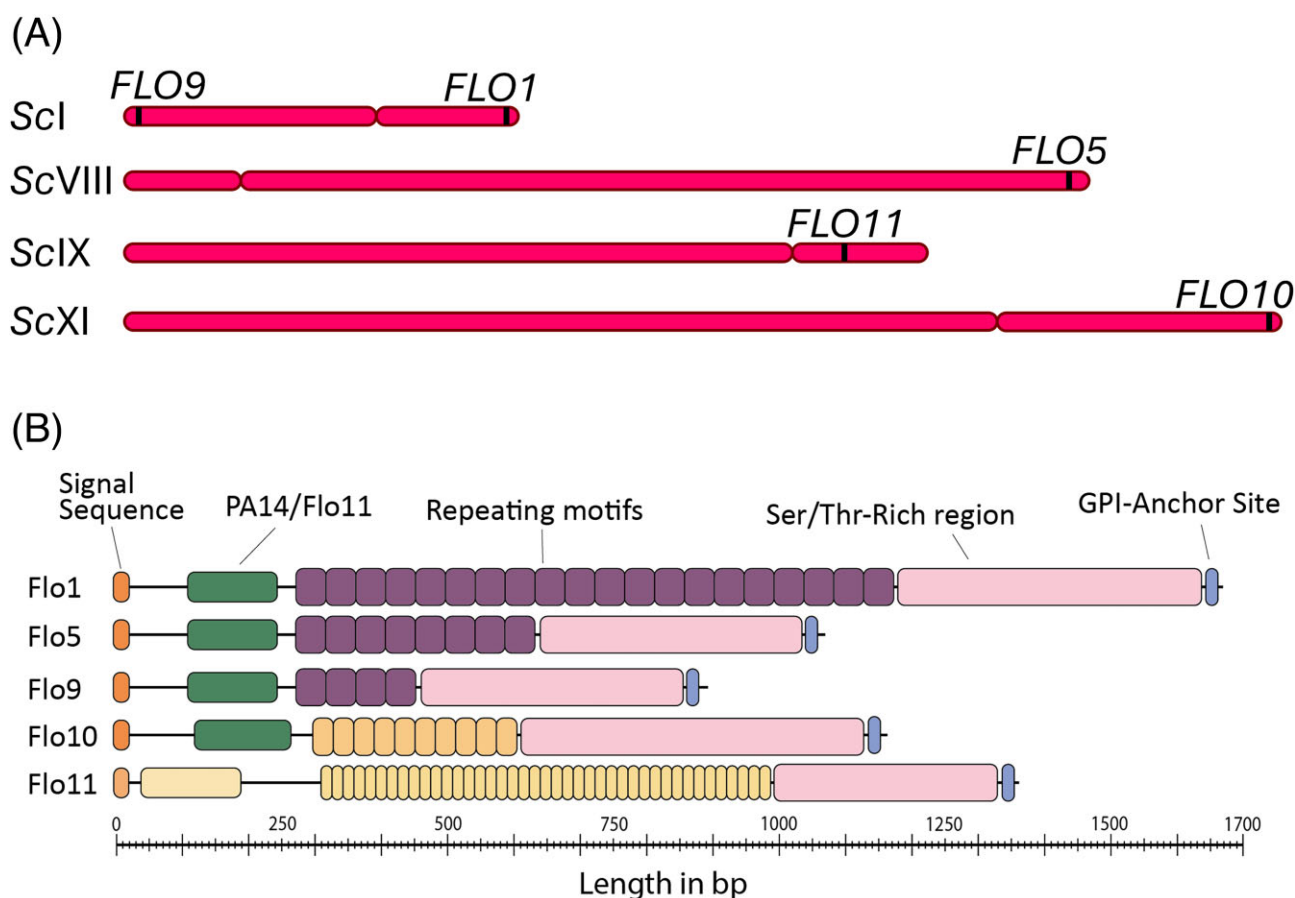


Figure 1. (A) Chromosomal locations of the *FLO* genes in *S. cerevisiae* strain CEN.PK113-7D based on the nanopore genome assembly (Salazar et al. 2017, van den Broek et al. 2023). *FLO1* and *FLO9* are located on the opposite ends of chromosome I. *FLO5* is located on chromosome VIII, *FLO11* on chromosome IX and *FLO10* on chromosome XI. Except for *FLO11*, all *FLO* genes are located in the subtelomeric region. (B) General structural motifs of Flo proteins found in the *S. cerevisiae* strain CEN.PK113-7D. All Flo proteins contain a signal sequence at the N-terminus, followed by a PA14 carbohydrate binding site (or the Flo11 domain), a series of repeating sequences, terminating with a GPI-anchor site at the C-terminus.

type (Verstrepen et al. 2005, Van Mulders et al. 2010, Tofalo et al. 2014).

Flocculation is regulated by a complex network of transcription factors (Robertson and Fink 1998, Pan and Heitman 2002), chromatin remodelling proteins (Halme et al. 2004), and epigenetic mechanisms (Rowlands et al. 2019). Key regulators include Flo8, a transcriptional activator (Fichtner et al. 2007) that cooperates with Mss11 and the Swi/Snf complex to activate *FLO* genes (Gagiano et al. 1999, Bester et al. 2006, Kim et al. 2014), and Sfl1, a repressor acting via the Tup1/Cyc8 co-repressor complex (Conlan and Tzamarias 2001, Ansanay Galeote et al. 2007). Additionally, High Osmolarity Glycerol (HOG) and Cell Wall Integrity (CWI) signaling pathways also activate flocculation. Under osmotic stress, Hog1 phosphorylation reduces Tup1/Cyc8 binding and promote active chromatin (Rowlands et al. 2019), while Rlm1 phosphorylation via Slt2 during cell wall stress, enables *FLO* genes activation (Sariki et al. 2019). In lager yeasts, the pH response regulator Rim101 influences flocculation (Zhou et al. 2021). *FLO* mRNA may also be regulated post-transcriptionally by Sen1 as proposed by Singh et al., (2015). Histone deacetylases and pleiotropic regulators, including Tup1 and Cyc8 (Keleher et al. 1992) further underscores the multifaceted control of flocculation (Wang et al. 2020). Despite advances, *FLO* gene redundancy, regulatory complexity, and the need for precise timing still challenge both understanding and engineering of this phenotypic trait in industrial applications.

To address this, we developed a *S. cerevisiae* platform strain lacking all native *FLO* genes. We then reintroduced individual *FLO* genes under precise temporal optogenetic control, allowing to dissect the roles of Flo1, Flo5, Flo9, Flo10 and Flo11 in floc formation, sugar sensitivity, and cell-surface hydrophobicity. This provides a robust framework for systematically characterizing flocculins and advancing our understanding of flocculation in *S. cerevisiae*, with implications for both fundamental biology and industrial biotechnology.

Materials and methods

Strains and growth conditions

The *S. cerevisiae* strains used in this study originate from the CEN.PK background (Entian and Kötter 2007) and are listed in Table 1. Yeast stocks were stored in 30% v/v glycerol at -80°C. Yeast cultures were inoculated from frozen stocks into 500 mL shake flasks containing 100 mL liquid YPD medium containing 10 g·L⁻¹ yeast extract, 20 g·L⁻¹ peptone and 20 g·L⁻¹ glucose, and incubated at 30°C in an Innova 44 incubator shaker (Eppendorf, Nijmegen, Netherlands) set at 200 rpm. For the flocculation tests, strains were inoculated in chemically defined medium (SMD) containing 20 g·L⁻¹ glucose, 3 g·L⁻¹ KH₂PO₄, 0.5 g·L⁻¹ MgSO₄·7H₂O, 5 g·L⁻¹ (NH₄)₂SO₄, 1 mL·L⁻¹ of a trace element solution and of a vitamin solution (Verduyn et al. 1992). For the selection of transfor-

Table 1. Strains used in this study.

Strain name	Genotype	Parental Strain	Origin
CEN.PK2-1C	MATa MAL2-8C his3Δ1 leu2-3, 112 trp1-289 ura3-52	–	Entian and Kotter 2007ence is already in the list. the citation in table
CEN.PK113-7D	MATa MAL2-8C	–	
IMI528	MATa MAL2-8c leu2-3, 112 trp1-289 ura3-52 HIS3::HIS3 _{cg} -pTEF1-VP16-EL222 ^{A79Q} -tCYC1, pC120-QF2-tACT1 p5xQUASf-GFP-tADH1 pCCW12-QS-PSD-tENO1)	CEN.PK2-1C	This study
IMX2600	MATa MAL2-8C can1Δ::Spycas9-natNT2	CEN.PK113-7D	van den Broek et al. 2023
IMK1041	MATa MAL2-8C can1Δ::Spycas9-natNT2 flo11Δ	IMX2600	This study
IMK1043	MATa MAL2-8C can1Δ::Spycas9-natNT2 flo10Δ flo11Δ	IMK1041	This study
IMK1044	MATa MAL2-8C can1Δ::Spycas9-natNT2 flo5Δ flo10Δ flo11Δ	IMK1043	This study
IMK1046	MATa MAL2-8C can1Δ::Spycas9-natNT2 flo5Δ flo9Δ::KanMX flo10Δ flo11Δ	IMK1044	This study
IMX1047	MATa MAL2-8C can1Δ::Spycas9-natNT2 flo1Δ::hphNT1 flo5Δ flo9Δ::KanMX flo10Δ flo11Δ	IMK1046	This study
IMK1060	MATa MAL2-8C can1Δ::Spycas9-natNT2 flo1Δ flo5Δ flo9Δ flo10Δ flo11Δ	IMK1047	This study
IMK1061	MATa MAL2-8C sfl1Δ	CEN.PK113-7D	This study
IMX2897	MATa MAL2-8C X-2:::(pTEF1_VP16-EL222 ^{A79Q} -tCYC1, pC120_QF2_tACT1, p5xQUASf_GFP_tADH1, pCCW12_QS_PSD_tENO1) can1Δ::Spycas9-natNT2 flo1Δ flo5Δ flo9Δ flo10Δ flo11Δ	IMK1060	This study
IMX2912	MATa MAL2-8C X-2:::(pTEF1_VP16-EL222 ^{A79Q} -tCYC1, pC120_QF2_tACT1, p5xQUASf_FLO1_tADH1, pCCW12_QS_PSD_tENO1) can1Δ::Spycas9-natNT2 flo1Δ flo5Δ flo9Δ flo10Δ flo11Δ	IMX2897	This study
IMX2913	MATa MAL2-8C X-2:::(pTEF1_VP16-EL222 ^{A79Q} -tCYC1, pC120_QF2_tACT1, p5xQUASf_FLO5_tADH1, pCCW12_QS_PSD_tENO1) can1Δ::Spycas9-natNT2 flo1Δ flo5Δ flo9Δ flo10Δ flo11Δ	IMX2897	This study
IMX2914	MATa MAL2-8C X-2:::(pTEF1_VP16-EL222 ^{A79Q} -tCYC1, pC120_QF2_tACT1, p5xQUASf_FLO9_tADH1, pCCW12_QS_PSD_tENO1) can1Δ::Spycas9-natNT2 flo1Δ flo5Δ flo9Δ flo10Δ flo11Δ	IMX2897	This study
IMX2915	MATa MAL2-8C X-2:::(pTEF1_VP16-EL222 ^{A79Q} -tCYC1, pC120_QF2_tACT1, p5xQUASf_FLO10_tADH1, pCCW12_QS_PSD_tENO1) can1Δ::Spycas9-natNT2 flo1Δ flo5Δ flo9Δ flo10Δ flo11Δ	IMX2897	This study
IMX2916	MATa MAL2-8C X-2:::(pTEF1_VP16-EL222 ^{A79Q} -tCYC1, pC120_QF2_tACT1, p5xQUASf_FLO11_tADH1, pCCW12_QS_PSD_tENO1) can1Δ::Spycas9-natNT2 flo1Δ flo5Δ flo9Δ flo10Δ flo11Δ	IMX2897	This study

mants, YPD medium was supplemented with G418 or Hygromycin B at concentrations of 200 mg·L⁻¹ and 100 mg·L⁻¹, respectively. For selection of the amdSYM marker, (NH₄)₂SO₄ was replaced by 0.6 g·L⁻¹ acetamide as nitrogen source and 6.6 g·L⁻¹ K₂SO₄ to compensate for sulfate in SMD resulting in SMD-AC (Solis-Escalante et al. 2013). For the selection of the integration of the optogenetics systems in the CEN.PK2-1C background, SMD medium was supplemented with leucine (500 mg·L⁻¹), tryptophan (75 mg·L⁻¹), and uracil (150 mg·L⁻¹) (Pronk 2002). The pH in all the media was adjusted to 6.0 with KOH. Solid media were prepared by adding 2% bacto agar to the abovementioned media.

To induce the optogenetic systems using blue light, a LED panel (HQRP New Square 12" Grow Light Blue LED 14 W) placed 30 cm above the cultures at the top of an Innova 44 incubator shaker (Eppendorf, Nijmegen, Netherlands) and Vattensten LED Strips (Ikea, Leiden, Netherlands) were used, which resulted in a light intensity between 20 and 40 μmol·m⁻²·s⁻¹ measured using a quantum meter (Apogee Instruments, Model MQ-510), allowing to count equally all photons in a wavelength between 400 and 700 nm. One μmol·m⁻²·s⁻¹ is about 6.02 x 10¹⁷ photosynthetically active radiation photons·m⁻²·s⁻¹. The shakers and shake flasks were covered to block ambient light (Figure S1).

Molecular biological techniques

Primers used in this study were ordered from Sigma-Aldrich (Burlington, MA) (Table S1). Fragments for genome integration

were amplified using Phusion High-Fidelity DNA polymerase (Thermo Fisher Scientific, Waltham, MA), diagnostic PCR used DreamTaq PCR Master Mix (Thermo Fisher Scientific). PCR products were purified with the Zymoclean Gel DNA Recovery Kit (Zymo Research, Irvine, CA) and were sequenced using Sanger sequencing (Macrogen Europe Amsterdam, the Netherlands). Plasmids were isolated using GeneJET Miniprep kit (Thermo Fisher Scientific) and Gibson assemblies were performed with NEB Gibson Master Mix (New England Biolabs, Ipswich, MA).

Plasmid construction

Plasmids used in this study are found in Table 2. For the targeting of FLO5, FLO10, FLO11 and GFP, the gRNA expressing plasmids pUDR834, pUDR825, pUDR827 and pUDR868 were constructed according to the protocol described by Mans et al. (2018). For the assembly of pUDR834, pUDR825, pUDR827, and pUDR868, the singular primers 19 225, 18 917, 18 918 and 19 736 were used for the amplification of each gRNA inserts from pROS backbones, respectively. The pROS11, pROS12 and pROS13 backbones were amplified using primer 6005 for the assembly of pUDR868 (pROS11), pUDR825 (pROS12), pUDR827 (pROS13) and pUDR834 (pROS13). Assembly was done using Gibson assembly. The pUD1305 plasmid was Gibson assembled from two fragments: a fragment containing an I-SceI overexpression cassette amplified with primers 19 671 and 19 672 using the plasmid pUDE206 as template (Solis-Escalante et al. 2013) and a second fragment

Table 2. Plasmids used in this study.

Name	Relevant characteristics	Purpose	Reference
pUDR834	2 μ m ori bla kanMX gRNA-FLO5 gRNA-FLO5	pROS13 expressing gRNA targeting FLO5	This study
pUDR825	2 μ m ori bla hphNT1 gRNA-FLO10 gRNA-FLO10	pROS12 expressing gRNA targeting FLO10	This study
pUDR827	2 μ m ori bla kanMX gRNA-FLO11 gRNA-FLO11	pROS13 expressing gRNA targeting FLO11	This study
pUD1305	ori bla AB-ISceI ^{TS} -AgTEF1p-AmdSYM-AgTEF1t-ISceI ^{TS} -AB	Constitutive expression of I-SceI with AmdSYM marker	This study
pUDR868	2 μ m ori bla amdSYM gRNA-GFP gRNA-GFP	Expression of gRNA targeting GFP	Mans et al. (2015)
pROS11	2 μ m ori bla amdSYM gRNA-CAN1.Y gRNA-ADE2.Y	Template to construct pUDR868	Mans et al. (2015)
pROS12	2 μ m ori bla hphNT1 gRNA-CAN1.Y gRNA-ADE2.Y	Template to construct pUDR825 & pUDR827	Mans et al. (2015)
pROS13	2 μ m ori bla kanMX gRNA-CAN1.Y gRNA-ADE2.Y	Template to construct pUDR834	Solis-Escalante et al. (2014)
pUDE206	2 μ m ori bla natNT1 TPI1p-I-SceI-TEF1t	Source of I-SceI expression cassette	Juergens et al. (2018)
pUD527	ori kanR AgTEF1p-amdSYM-AgTEF1t	Source for amdSYM expression cassette	Gorter de Vries et al. (2019)
pUDP104	ori bla panARS ^{opt} amdSYM Spycas9 gRNA-ScSFL1	Expression of gRNA targeting SFL1	Bouwknegt et al. (2021)
pUDR538	2 μ m bla hphNT1 gRNA-X-2.Y	Expression of gRNA targeting X-2 locus	Solis-Escalante et al. (2014)
pDS1	AB-ISceI ^{TS} -KanMX-ISceI ^{TS} -AB	Contains KanMX marker flanked by I-SceI sites	Solis-Escalante et al. (2014)
pDS7	AB-ISceI ^{TS} -AgTEF2p-hphNT1-AgTEF2t-ISceI ^{TS} -AB	Contains hphNT1 marker flanked by I-SceI sites	Lalwani et al. (2021)
pMAL724	ori bla HIS3cg_(pTEF1_VP16-EL222 ^{A79Q} _tCYC1, pC120_QF2_tACT1,p5xQUASf_GFP_tADH1, pCCW12_QS_PSD_tENO1)	Contains OptoQ-AMP5	

containing the amdSYM marker obtained through PCR amplification with primers 3847 and 3276 using the plasmid pUD527 as template. The resulting fragments are flanked by A and B SHR sequences (Kuijpers et al. 2013) and assembled into pUD1305.

Strain construction

Integration of optogenetics system

The OptoQ-AMP5 (Lalwani et al. 2021) was integrated into the HIS3 locus of CEN.PK2-1C as originally described in (Zhao et al. 2018) using the plasmid pMAL724 (Addgene plasmid #169 151) (<https://www.addgene.org/>), resulting in the strain IMI528.

The FLO-null strain IMX1060

The IMK1060 (FLO-null strain) was constructed through serial transformations knocking out each FLO gene consecutively using a combination of CRISPR Cas9 and homology directed repair-mediated deletions as described by Mans et al. (2015) and Solis-Escalante et al. (2014), respectively. All transformations were performed according to the lithium acetate protocol described by Gietz and Woods (2002). IMX2600 (van den Broek et al. 2023) was first transformed with the plasmid pUDR827 and the repair DNA fragment made of the annealing of the complementary primers 18 933 and 18 934 to remove FLO11, resulting in the strain IMK1041. Then, FLO10 was removed by transformation with pUDR825 and the corresponding repair DNA consisting of primers 18 931 and 18 932, resulting in the strain IMK1043. FLO5 was subsequently removed by transformation with pUDR834 and the corresponding repair DNA consisting of primers 19 236 and 19 237 to create the strain IMK1044. Due to difficulties targeting FLO1 and FLO9 using CRISPR-Cas9 system, a classical approach based on introduction of PCR-based deletion cassette by homology directed repair was used (Wach et al. 1994). For the deletion of FLO9, a repair fragment containing the hygromycin resistance marker was PCR amplified from the pDS7 plasmid using the primers 19435 and 19436, while for FLO1, a repair fragment containing the G418 resistance marker was PCR amplified from the plasmid pDS1 using

primers 19433 and 19434. Transformation was performed using 1 μ g of PCR product and selection was performed on YPD supplemented with the required antibiotics. First, FLO9 was knocked out by introduction of the PCR-amplified KanMX repair fragment by homology directed repair, resulting in the strain IMK1046. FLO1 was then knocked out in this strain by introducing the hphNT1 repair fragment, creating the strain IMK1047. Finally, a final transformation was performed with the pUD1305 plasmid containing the I-SCEI and the AnamdS genes. Selection was done on SM-Ac plates and successful transformants were screened for loss of resistance on YPD with and without supplemented antibiotics. One colony was verified using PCR (Figure S2), stocked and sequenced to confirm the successful removal of all FLO genes and the resistance markers. The resulting strain IMK1060 was dubbed the FLO-null strain (Figure 2). SFL1 was deleted in CEN.PK113-7D using the gRNA plasmid pUDP104 and repair primers 18 937 and 18 938 as described in the protocol of Mans et al. (2018).

Construction of Opto-FLO strains

OptoQ-AMP5 system was inserted into IMK1060 genome at the X-2 locus (Mikkelsen et al. 2012) using pUDR538 and two overlapping repair fragments amplified from pMAL724 with SHR-A (Kuijpers et al. 2013) and X-2 flanks. Resulting strain IMX2897 (flo Δ X-2::OptoQ-AMP5) served as the optogenetic platform. The X-2 integration site is located on the left arm of CHR_X between the NCA3 and ASF1 genes. The spacer sequence used to target X-2 site is comprised between position 195 626 and 195 624 (position based on S288c genome). Each FLO gene was fused with OptoQ elements using 60 bp arms homologous to the 5xQUASfp and ADH1t regions and integrated via CRISPR-Cas9 using pUDR868 and repair fragments, yielding strains IMX2912–IMX2916. Insertion was confirmed by PCR and amplicon sequencing. The primer pairs 19988/19989, 19990/19991, 19992/19993, 19994/19995 and 19996/19997 were designed for FLO1, FLO5, FLO9, FLO10, and FLO11, respectively.

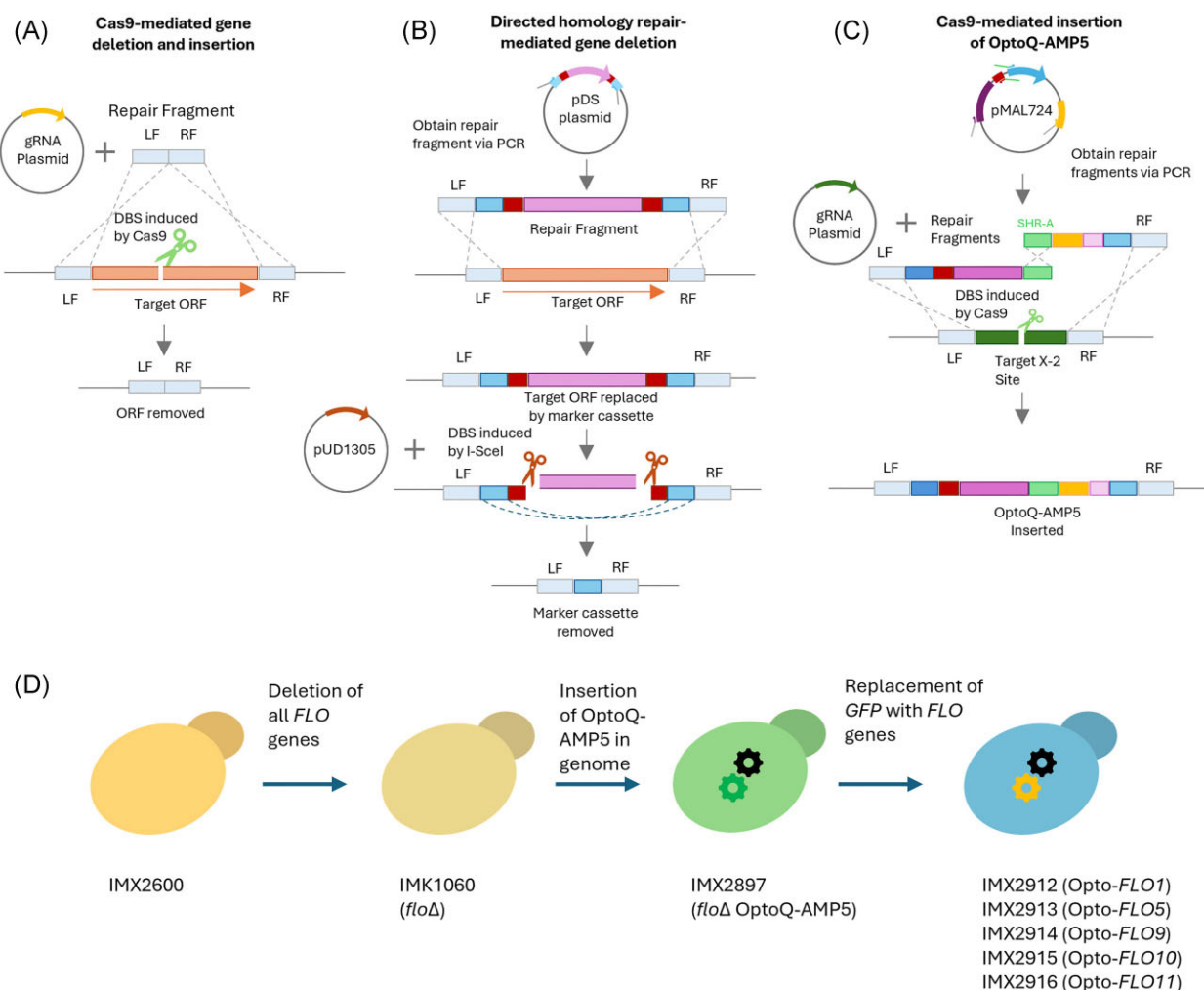


Figure 2. Gene deletion strategies were employed to create the *FLO*-null strain (IMK1060). **(A)** Deletion of *FLO5*, *FLO10* and *FLO11* using CRISPR-Cas9 mediated homologous recombination. A 120 bp repair fragment replaces the *FLO* gene open reading frame, resulting in a knockout of the gene. **(B)** Deletion of *FLO1* and *FLO9* using homology directed repair to replace the open reading frame with antibiotics-resistance cassettes. The markers are subsequently removed by I-SceI-mediated homologous recombination. **(C)** Insertion of the OptoQ-AMP5 system into the X-2-locus (Mikkelsen et al. 2012) using Cas9-mediated homologous recombination. **(D)** Overview of the strain engineering strategy. For the insertion of the *FLO* genes at the GFP locus in the OptoQ-AMP5 system, the same strategy as in **(C)** was used using flanks homologous to the promoter and terminator flanking GFP.

Determination of fluorescence using flow cytometry

CEN.PK113-7D and IMI528 were grown in 500-mL shake flasks containing 100 mL SMD medium at 30°C at 250 rpm in duplicates under light and dark conditions. First, each strain was inoculated from a -80°C glycerol stock and grown overnight in YPD in full darkness. The strains were transferred to SMD at an OD_{660nm} of 0.1 and grown for approximately 8 hours in full darkness. From this culture, duplicate experimental cultures were inoculated using a calculated amount of cells in 100 ml fresh SMD so that the OD_{660nm} would reach 4 after approximately 16 hours of growth. Once the OD_{660nm} reached 4, one set of duplicates for each strain was grown under light conditions while the other set remained under dark conditions. One ml samples were taken from cultures growing under blue light at different time points from the start of the induction. The samples were analysed by measuring the fluorescence levels using the BD Accuri™ C6 CSampler Flow Cytometer (BD Biosciences, Franklin Lakes, NJ). The GFP was excited with the 488 nm laser of the flow cytometer and emission was

detected through a 533 nm bandpass filter with a bandwidth of 30 nm. For each sample, 100.000 events were measured. The forward scatter (FSC) and side scatter (SSC) were plotted and gated to remove particles with outlying sizes. The median fluorescence was determined using the gated cells.

Growth rate determination

Strains were grown in 500-mL shake flasks containing 100 mL SMD medium at 30°C at 250 rpm in triplicates under light and dark conditions. Each strain was inoculated from a -80°C glycerol stock and grown overnight in YPD in full darkness. The strains were then transferred to SMD at an OD of 0.1 in full darkness. From this culture, the experimental cultures were inoculated at a starting OD₆₆₀ of 0.1 in triplicates. Samples were taken during the exponential phase and the OD₆₆₀ was determined using a Jenway 7200 scanning spectrophotometer (Cole-Parmer Inc, Chicago, MI). Maximum specific growth (μ_{max}) rate was calculated from the slope of log transformed OD_{660nm} data across at least six points.

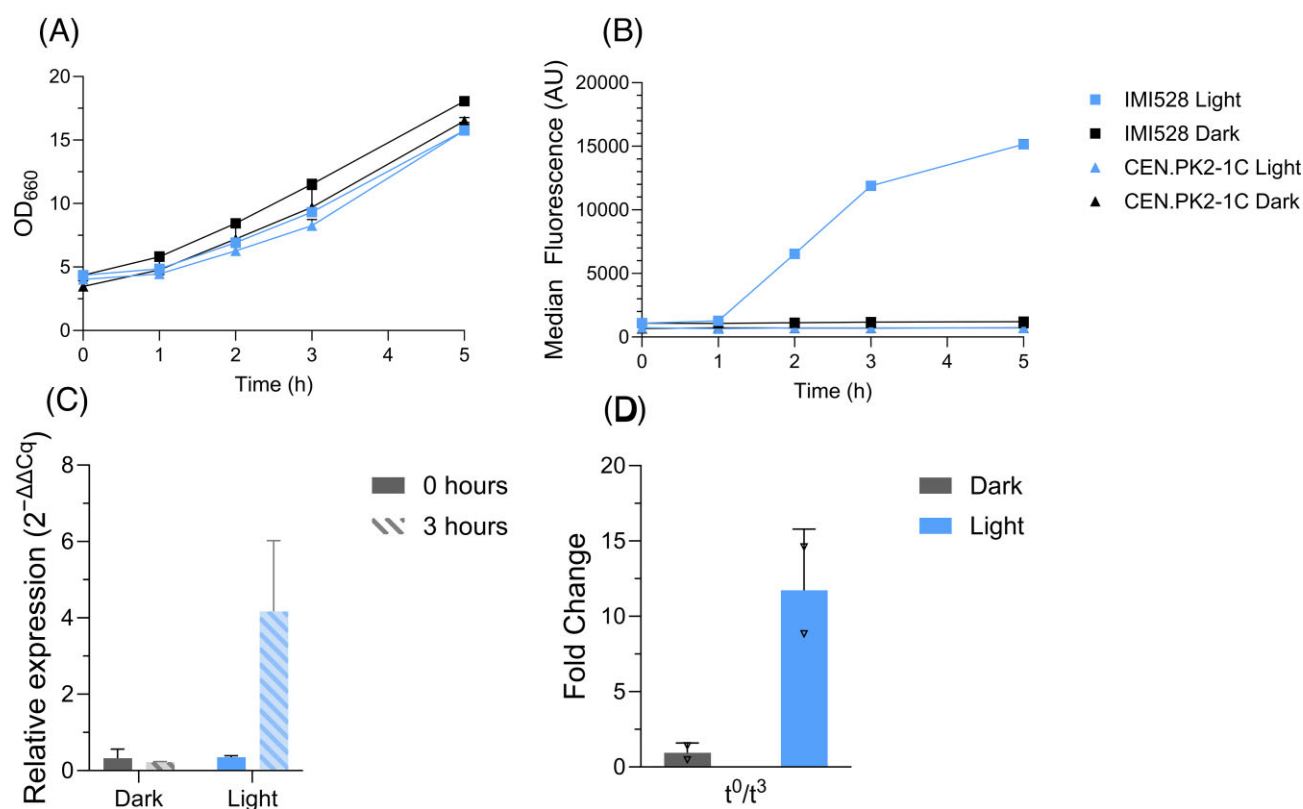


Figure 3. Growth of IMI528 and CEN.PK2-1C under light and dark conditions. The cultures were induced with light or grown in darkness mid exponential phase for 5 hours. **(A)** Growth curve of strains grown under light and dark conditions for 5 hours. **(B)** Median fluorescence levels of strains in light and dark condition. After 1 hour of induction, only a minor increase was observed relative to $t = 0$ for IMI528. After 3 hours, the fluorescence increased by 11-fold, while after 5 hours the fluorescence started to plateau at 14-fold increase relative to $t = 0$. IMI528 showed a consistently higher median fluorescence under dark conditions relative to CEN.PK2-1C. **(C)** Relative expression values of GFP compared to the geocentric mean of *ALG9*, *UBC6* and *TFC1* at $t = 0$ and $t = 3$ for IMI528. A 4-fold increase relative to the control was observed under light conditions at $t = 3$, while no difference was observed at $t = 0$ between the light and dark samples. **(D)** Fold change in expression of GFP over $t = 3$ relative to $t = 0$. A 12x fold change in gene expression was observed at $t = 3$ relative to $t = 0$, matching the observed fold change in fluorescence.

RNA extraction and quantitative RT-PCR

Samples were taken during exponential phase and quenched directly in liquid nitrogen. Cells were lysed mechanically and total RNA was extracted with acid-phenol:chloroform (pH 4.5 with IAA, 125:24:1) and ethanol precipitation (Tai et al. 2005). The concentration, integrity and purity of the samples were determined using the Qubit (Thermo Fischer Scientific), Tapestation 220 with RNA Screen Tape (Agilent Technologies) and Nanodrop (Thermo Fischer Scientific), respectively. DNA was removed using RNase-Free DNase (Promega, Madison, WI).

To determine the expression levels of GFP by the optogenetics system in light and dark conditions, a qRT-PCR reaction was performed. cDNA synthesis and qRT-PCR were performed using the GoTaq® 2-Step RT-qPCR kit (Promega) with 500 ng RNA input. cDNA was normalised to 35 ng·μL⁻¹. The primers used for the qRT-PCR reactions were designed using Clone Manager (version 9.51, Sci-Ed Software, Denver, CO) and diluted to a concentration of 2 μM in the reaction mix. Optimal annealing temperatures was determined to be 68°C using a gradient qPCR. Reference genes included *UBC6*, *TFC1* and *ALG9* (Teste et al. 2009). Data were analyzed using the Livak (2^{-ΔΔCq}) method for relative gene expression analysis. Reactions were run in triplicate on a qTOWER³ instrument with inter-plate calibrators.

Flo sequence analysis

The DNA and protein sequences of the *FLO* genes of *Saccharomyces cerevisiae* CEN.PK113-7D and S288C were obtained from the annotated assembly of CEN.PK113-7D (accession: PR-JNA393501,) and SGD (Saccharomyces Genome Database, <http://www.yeastgenome.org/>) (Grünler et al. 2010, Salazar et al. 2017), respectively. Protein sequences were aligned using Clustal Omega 1.2.4 (Sievers and Higgins 2018). Protein domains were identified using the Interpro database (Blum et al. 2024). Repeating motifs were identified using a combination of methods. First, the protein sequences were used as input in RADAR (Madeira et al. 2024) to identify potential repeating motifs. Based on these results, the protein sequence was trimmed into sections containing unique repeating motifs and each section was inputted again into RADAR. The repeat sequences were aligned using Clustal Omega 1.2.4 and redefined based on the alignment output. A consensus sequence was determined using the EMBOSS Cons tool (Madeira et al. 2024).

Microscopy

Image acquisition was conducted using a Zeiss AXIO Imager.Z1 microscope (Carl Zeiss AG, Oberkochen, Germany). The floc structure of IMX2897 (*floΔ X-2::OptoQ-AMP5*) and the induced strains (IMX2912, IMX2913, IMX2914, and IMX2915) was explored by taking samples from the sedimented cells following the flocculation assay. Microscopic analysis of fractions was performed using Zeiss

Table 3. Overview of the relevant domains and repeating motifs of Flo proteins identified in *S. cerevisiae* CEN.PK113-7D and S288C strains.

Species	Strain	Protein	Length(AA)	Signal sequence	PA14/Flo11	Central domain	GPI anchor site	Residue	Repeat type 1	Repeat type 2	Repeat type 3	Repeat type 4	Repeat type 5
<i>S. cerevisiae</i>	CEN.PK113-7D	Scl-Flo1	1675	1-24	112-248	274-1173	1652	G	20	13	2	3	5
<i>S. cerevisiae</i>	CEN.PK113-7D	Scl-Flo9	959	1-24	112-248	274-453	936	G	4	13	4	3	2
<i>S. cerevisiae</i>	CEN.PK113-7D	ScVIII-Flo5	1075	1-24	112-247	274-633	1052	G	8	6	2	3	2
<i>S. cerevisiae</i>	CEN.PK113-7D	ScIX-Flo11	1367	1-21	31-207	313-879	1346	G	41*	7*	2*	-	-
<i>S. cerevisiae</i>	CEN.PK113-7D	ScXI-Flo10	1169	1-24	123-270	302-606	1352	G	10*	2*	3	2*	-
<i>S. cerevisiae</i>	S288C	Scl-Flo1	1537	1-24	112-248	274-1083	1514	G	18	6	2	3	4
<i>S. cerevisiae</i>	S288C	Scl-Flo9	1322	1-24	112-248	274-858	1299	G	13	9	2	3	3

Relevant domains were identified using the Interpro database (Blum et al. 2024). Repeating motifs were identified using RADAR, Clustal Omega 1.2.4 and manual curation as described in the methods section. Flo5, Flo10 and Flo11 were identical in CEN.PK113-7D and S288C. The Flo10 repeat types 1, 3 and 5 are unique compared to the other Flo1-like proteins. Flo11 is dissimilar to the Flo1-like proteins and contains unique repeating sequences. Unique motifs are marked with an asterisk (*).

ZENBlue software (Carl Zeiss AG). Cells were imaged at 200x and 400x magnification for floc size analysis.

Flocculation assays

A modified flocculation protocol based on the Helm's test (D'Hautcourt and Smart 1999) was developed (Figure S3). The tested strains were inoculated from a freezer stock in 100 mL YPD and after cultivation to an OD₆₆₀ of at least 10, the cells were transferred to 100 mL fresh SMD medium at a concentration reaching an OD₆₆₀ of 10 at the start of the next growth phase. Then, the cells were transferred to fresh SMD at a starting OD₆₆₀ of 3 and grown to an OD₆₆₀ of 5 in full darkness to ensure that all cells were in exponential phase. Once an OD₆₆₀ of 5 was reached, one set of shake flask cultures was exposed to blue light of 465 nm for 2 hours, while the other set of cultures grew in darkness. After two hours, cells were harvested, washed and subjected to a modified Helm's test. Cells were washed with a 50 mM EDTA solution, followed by washing with demineralised water and finally suspended in flocculation buffer (50 mM sodium acetate, pH 4.5) to reach an OD₆₆₀ of 10. The OD_{660nm} was determined (Value A, equation 1). Then, 6 ml cell suspension was transferred to glass tubes in triplicate and supplemented with 300 µl of 20% (w/v) CaCl₂, reaching a final concentration of 1%. The cells were immediately vortexed for 30 seconds, followed by a 15 minute gentle agitation step using a nutating mixer (VWR International, Radnor, PA). Then, the suspension was incubated upright for 5 minutes to allow for the sedimentation of the biomass. Samples were taken by aspirating 100 µl from under the meniscus, diluting in 900 µl 50 mM EDTA and measuring the OD₆₆₀ (Value B, equation 1). Additionally, a sample was taken for microscopic analysis. The relative difference in OD₆₆₀ between the deflocculated and sedimented samples can be calculated as the flocculation coefficient (equation 1). For the sugar inhibition assay, the same protocol was utilised with minor modifications (Figure S3), according to the method used by Van Mulders et al. (2009). At step 4, flocculation buffer was additionally supplemented with sugars at the concentrations of 20 mM, 100 mM, 500 mM and 1000 mM. Additionally, a sugar mix comprising 2.5% glucose, 28.0% maltose, 42.0% maltotriose, and 26.4% higher saccharides (w/w) was utilised at concentrations 10.1, 50.4, 252.2 and 504.4 g·L⁻¹, corresponding to approximately 20, 100, 500 and 1000 mM of sugars. The non-flocculent strain IMX2916 (*floΔ* X-2::OptoQ::FLO11) was not included in the inhibition assay.

$$\frac{A - B}{A} \cdot 100 = \text{flocculation coefficient} \quad (1)$$

Hydrophobicity assessment

For the determination of cell surface hydrophobicity, a modified protocol based on the method outlined by Rosenberg (1984) was used (Figure S3). Cells were harvested from cultures grown in light and dark conditions and subsequently washed with 50 mM EDTA to ensure deflocculation before the determination of the OD₆₆₀. A predetermined quantity of yeast cells was subjected to a wash step with 50 mM EDTA followed by demineralised water and then resuspended in 5 mL of 50 mM sodium acetate solution in Hungate tubes (Chemglass Life Sciences LLC, Vineland, NJ) to achieve an OD₆₆₀ of approximately 1. The OD₆₆₀ was determined (value A, equation 2). The yeast suspension was then overlaid with 1 mL of the hydrophobic hydrocarbon dodecane and vortexed at maximum speed for 60 seconds. The tubes were then placed upright upside down to allow for a 10 minute phase separation period. Following this period, the OD₆₆₀ of the aqueous layer was measured again by sampling through the septum using a needle (Value C,

Table 4. The consensus sequences of each type of repeating motif identified in the CEN.PK113-7D Flo proteins.

Repeat type	Consensus sequence	Length	Ser (%)	Thr (%)	Ser/Thr (%)
Flo1 Repeat type 1	gtITTTTTEPWTGFTFTSTSTEMTTVTGTNGQPTDETIVIVIRTPTE	45	4.4	42.2	46.7
Flo1 Repeat type 2	SSLPPVTSATTSSQETt	16	25.0	31.3	56.3
Flo1 Repeat type 3		51	11.8	29.4	41.2
	QTTTLVTVTSCEsXVCSETASPAIVSTATATVNGVTTEYTTWCPISTTEtTK				
Flo1 Repeat type 4	NTGAAETTT	9	0.0	44.4	44.4
Flo1 Repeat type 5	SVISS	5	60.0	0.0	60.0
Flo10 Repeat Type 1	TSSsXSSSEVCTECTETESTSyvTPYVxxxxxxxxxx	36	22.2	16.7	38.9
Flo10 Repeat Type 2	TTSkDStVgssTSsVsLiSSstssiSlpsSySAS	34	50.0	14.7	64.7
Flo10 Repeat Type 4	SEAaeTKSiSrmnnfVptS	19	21.1	10.5	31.6
Flo11 Repeat Type 1	PVPTPSSSTTESSSA	15	40.0	20.0	60.0
Flo11 Repeat Type 2	TTxVTTAVxTTITTECSTGTNSAGETTSGCsXKtlxTTxxTTx	44	9.1	40.9	50.0

Capital and lowercase letters indicate highly conserved and variable amino acids respectively. A consensus sequence was determined using the EMBOSS Cons tool (Madeira et al. 2024).

equation 2). This way, the organic layer could be avoided completely. The percentage of hydrophobicity was calculated as the relative change in absorbance of the aqueous layer before and after vortexing (equation 2).

$$\frac{A - C}{A} \cdot 100 = \text{Hydrophobicity percentage}$$

(2)

Whole genome sequencing

The genomic DNA of the strains IMK1060, IMX2897, IMX2912, IMX2913, IMX2914, IMX2915 and IMX2916 was isolated using the QIAGEN Genomic DNA isolation buffer set in combination with the Genomic-tip 100/G columns (Qiagen, Hilden, Germany) according to the manufacturer's instructions. All genomic DNA samples, except of IMX2914, were sequenced using a 150 bp Truseq PCR free library preparation with 300 bp insert on a Novaseq 6000 sequencer (Macrogen Europe, Amsterdam, The Netherlands). The raw Illumina reads were mapped using the Burrows–Wheeler Alignment tool (BWA) (Li 2013) against a chromosome-level reference genome of IMX2600 (NCBI bioproject accession number PRJNA976676 (<https://www.ncbi.nlm.nih.gov/bioproject/PRJNA976676>) (van den Broek et al. 2023). For the IMK1060 strain, 2 extra contigs were added containing the I-SceI-hphNT1 and I-SceI-KanMX resistance cassettes. For the remaining strains, an alignment was performed on the same reference and a separate contig containing the OptoQ-AMP5 sequence with or without the relevant FLO gene insertion. The strain IMX2914 was not sequenced, instead, the optogenetic cassette including ScFLO9 was PCR amplified using primers 19907 and 14455 and the resulting fragment was amplicon sequenced using nanopore technology (Oxford Nanopore, Oxford, United Kingdom) by Plasmidsaurus (South San Francisco, CA). Sequencing data are available at the NCBI repository (<https://www.ncbi.nlm.nih.gov/>) under Bioproject PRJNA1281879 (Table S2).

Results

Evaluation of the inducibility of the OptoQ-AMP5 optogenetic circuit

To capture the temporality of flocculation events in *Saccharomyces cerevisiae*, individual flocculins have to be expressed under an inducible promoter allowing precise control of flocculation onset. Classical inducible promoters, such as the galactose-inducible GAL1, GAL10, and GAL7 promoters (Hovland et al. 1989); maltose-inducible MAL promoters (Weinhandl et al. 2014); or the copper-inducible CUP1 (Hottiger et al. 1994), require medium modifica-

tions that may influence flocculation. To avoid this, we selected the OptoQ-AMP5 light inducible system (Lalwani et al. 2021), which uses the blue-light-activated VP16-EL222 transcription factor (TF), its target promoter C120p, the transcription factor QF2, and the chimeric CYC1p_{5xQUAS} promoter, which controls the expression of the gene encoding GFP. In darkness, the constitutively expressed light-responsive VP16-EL222 TF remains dissociated and is unable to induce downstream gene expression, thereby preventing GFP production. Upon exposure to blue light, VP16-EL222 undergoes dimerization and initiates a transcriptional cascade, leading to the expression of QF2 TF. QF2 subsequently binds to the CYC1p_{5xQUAS} promoter, activating GFP expression. The OptoQ-AMP5 system (pMAL724 (Lalwani et al. 2021)) was integrated into the his3Δ1 locus of strain CEN.PK2-1C, resulting in strain IMI528 (HIS3::OptoQ-AMP5). To test its functionality, IMI528 was grown in SMD and exposed to blue light (463 nm) for 5 hours in mid-exponential phase (Figure 3). Fluorescence stayed low and constant during the first hour, then rose rapidly, reaching a 13.8-fold increase after 5 hours. In darkness, fluorescence changed by only 10%. The negative control strain CEN.PK2-1C exhibited low fluorescence under both conditions. In darkness, IMI528 showed slightly higher fluorescence (p < 0.01) than CEN.PK2-1C, suggesting minor circuit leakiness. A two hours induction was sufficient for half-maximal activity.

To confirm fluorescence reflected gene expression, qPCR analysis (Heid et al. 1996, Winer et al. 1999) was performed at the 3 hours timepoint of IMI528 growth curve (Figure 3C & D). The Livak (2^{-ΔΔCT}) method (Livak and Schmittgen 2001) was utilised for the analysis of GFP expression relative to the geometric mean of three reference genes, namely ALG9, UBC6 and TFC1 (Teste et al. 2009). GFP exhibited an 11.7-fold increase in expression at t = 3 relative to t = 0 under light conditions, while exhibiting a 0.94 fold increase under dark conditions. Thus, GFP fluorescence reliably reported transcript levels.

Sequence analysis of flocculins of the *S. cerevisiae* strain CEN.PK113-7D

To examine FLO genes variation, Flo protein sequences from CEN.PK113-7D genome sequence (Salazar et al. 2017) were compared with S288C. Flo5, Flo10, and Flo11 were identical, but Flo1 and Flo9 differed in size (Tables 3 and 4). Flo1_{CEN.PK113-7D} was 138 amino acids longer and Flo9_{CEN.PK113-7D} was 363 amino acids shorter than in S288C, mainly due to differences in repeat numbers (Bernardi et al. 2018; Li 2013; Verstrepen et al. 2005) (Tables 3 and 4).

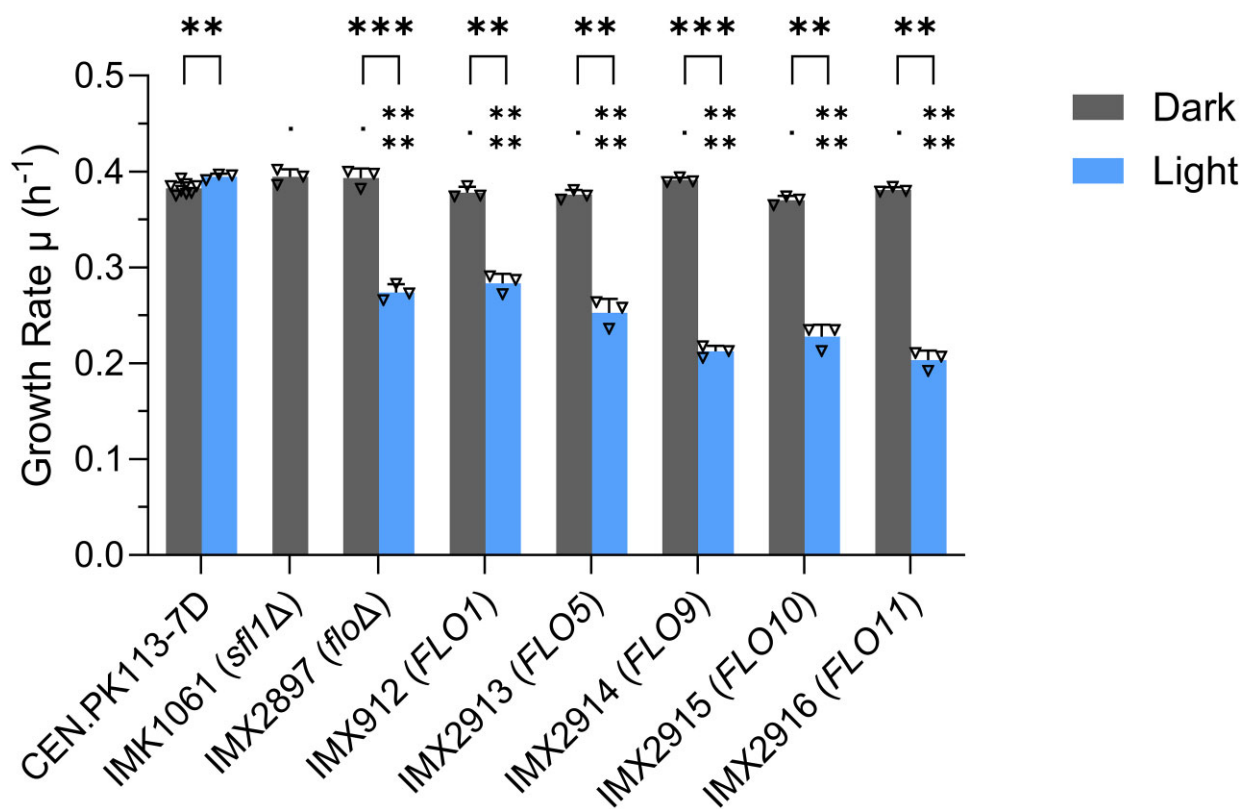


Figure 4. Maximum specific growth rates of CEN.PK113-7D, IMK1061, IMX2897 (*floΔ* X-2::OptoQ-AMP5), IMX2912, IMX2913, IMX2914, IMX2915 and IMX2916 grown under constant light and dark conditions. Symbols with brackets represent comparison between light and dark conditions per strain, while symbols without brackets represent a comparison to the CEN.PK113-7D (Dark) as reference. The growth rate of all strains grown under light was significantly reduced relative to dark conditions (** $p < 0.01$, *** $p < 0.001$). All strains grown under dark conditions showed no significant difference in growth rate compared to CEN.PK113-7D (dark), while the strains in light conditions had significantly lower growth rates (**** $p < 0.0001$). Each bar represents the average of 3 replicate cultures, except for the CEN.PK113-7D under dark conditions, which represents the controls of multiple growth experiments, totalling in 8 values. Each open triangle represents a datapoint. Error bars represent the standard deviation. Statistical significance was calculated using multiple unpaired two sided t-tests. P-values were corrected for multiple comparisons using the Holm-Šidák method.

Repeat analysis revealed five motifs in Flo1 (Table 3), including previously reported type 1 (Pfam: PF00624) and type 3 (Pfam: PF13928) (Goossens and Willaert, 2010), plus the presence of type 2, type 4 repeats, and a novel five-amino-acid serine-rich (SVISS) repeat. These motifs also appeared in Flo5 and Flo9 in different proportions (Table 3). Flo10 contained distinct types 1, 2, and 4, but lacked the SVISS repeat (Tables 3 and 4). The type 1 repeats dominated flocculins, except in Flo9, where type 2 repeats prevailed. All repeats were rich in serine and threonine residues (31% to 65%) (Table 4) known for O-glycosylation, which stabilises proteins (Caro et al. 1997; K. Goossens and Willaert, 2010; Straver et al. 1994; Teunissen et al. 1993) and projects the PA14 domain above the cell wall (Jentoft 1990). Repeat variations likely influences floc stability and binding ability. Despite differences in repeat numbers, overall Ser/Thr content was consistent (~40% for Flo1-type adhesins and ~50% for Flo11). These findings highlight how architectural variation impacts function despite sequence similarity.

Construction of a *S. cerevisiae* FLO-null strain and optogenetic dependent single flocculin expressing derived strains

S. cerevisiae carries five FLO genes, FLO1, FLO5, FLO9, FLO10 and FLO11 (Figure 1). FLO1, FLO5, FLO9, and FLO10 mediate aggregation, while FLO11 is involved in pseudohyphal growth (Verstrepen et al. 2004). Prior studies often used strains retaining native FLO genes (Bidard et al. 1994, Stratford 1994, Govender et

al. 2008, Van Mulders et al. 2009, Deed et al. 2017, Di Gianvito et al. 2017) risking interference. To avoid this, we constructed a FLO-null (IMK1060) via sequential CRISPR-Cas9 deletions of FLO5, FLO10, FLO11, and traditional gene interruption through homology directed repair of FLO1 and FLO9, including I-SceI recycling of the PCR amplified deletion cassette carrying KanMX and hphNT1, respectively (Solis-Escalante et al. 2014) (Figure 2). In a second step, the OptoQ-AMP5 system was integrated into the X-2 locus on CHR X (Mikkelsen et al. 2012) (Figure 2), yielding IMX2897 (*floΔ* X-2::OptoQ-AMP5). Replacing GFP with each FLO gene generated IMX2912 (*floΔ* X-2::OptoQ::FLO1), IMX2913 (*floΔ* X-2::OptoQ::FLO5), IMX2914 (*floΔ* X-2::OptoQ::FLO9), IMX2915 (*floΔ* X-2::OptoQ::FLO10) and IMX2916 (*floΔ* X-2::OptoQ::FLO11).

Flo protein characterisation using the optogenetic circuit OptoQ-AMP5

Growth rates of FLO-expressing strains were measured under light and dark conditions in triplicate in SMD medium (Figures 4 and S4). Control strain CEN.PK113-7D grew at $0.38 \pm 0.006 \text{ h}^{-1}$ and $0.39 \pm 0.003 \text{ h}^{-1}$ in dark and light conditions respectively (Kuyper et al. 2005), while the flocculating control strain IMK1061 (*sf1Δ*) grew similarly in dark and light ($0.38 \pm 0.006 \text{ h}^{-1}$ and $0.039 \pm 0.008 \text{ h}^{-1}$). In contrast, all OptoQ-AMP5 strains exhibited reduced growth rates under blue light: a 25% reduction for IMX2912 (*floΔ* X-2::OptoQ::FLO1) and up to 46% for IMX2914 (*floΔ* X-2::OptoQ::FLO9). The strains IMX2916 (*floΔ* X-2::OptoQ::FLO11)

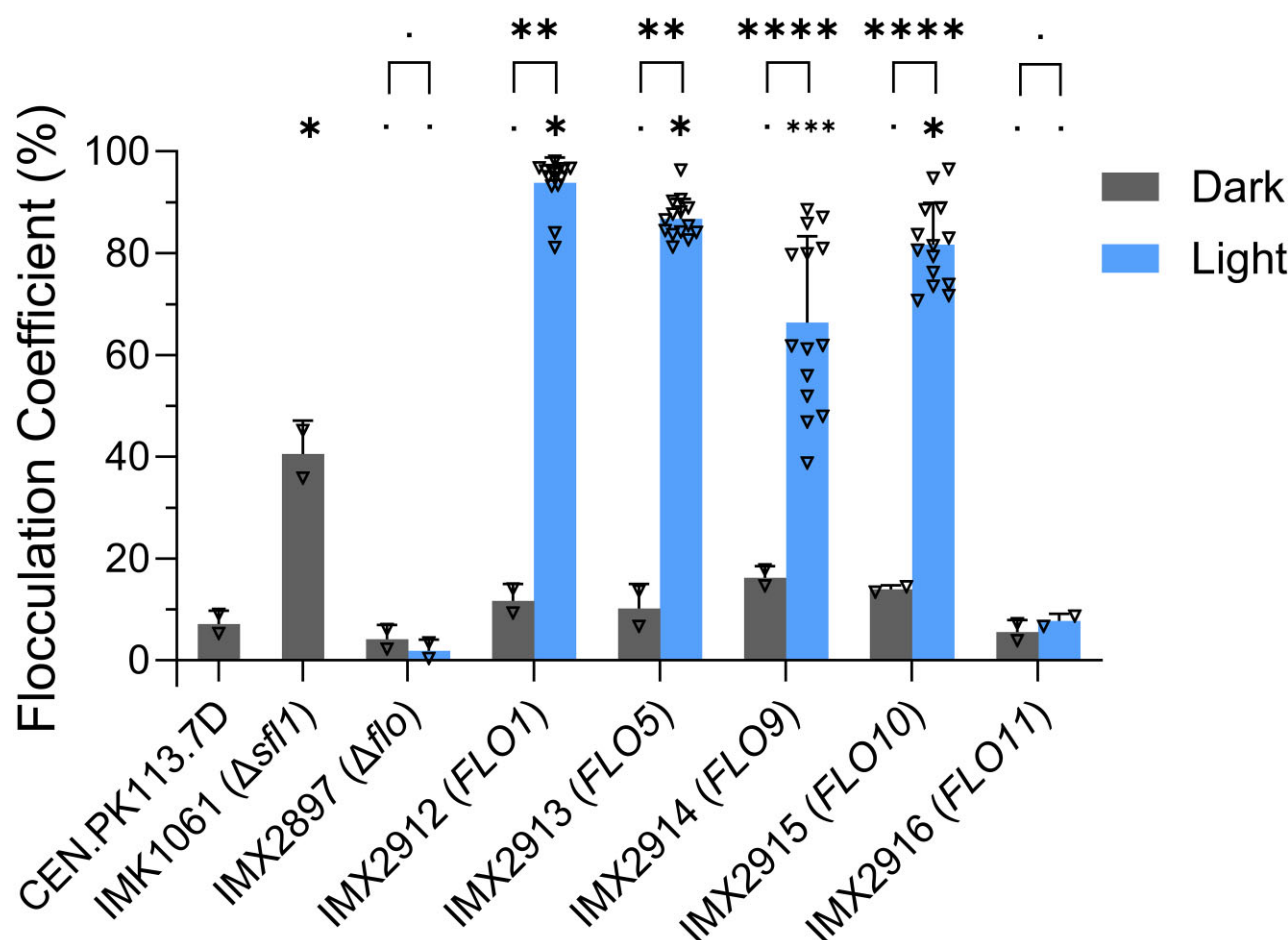


Figure 5. Flocculation coefficient of CEN.PK113-7D, IMK1061 (*sf1Δ*), IMX2897 (*floΔ X-2::OptoQ::AMP5*), IMX2912 (*floΔ X-2::OptoQ::FLO1*), IMX2913 (*floΔ X-2::OptoQ::FLO5*), IMX2914 (*floΔ X-2::OptoQ::FLO9*), IMX2915 (*floΔ X-2::OptoQ::FLO10*) and IMX2916 (*floΔ X-2::OptoQ::FLO11*) grown under dark and light conditions for two hours in exponential phase. The flocculation coefficient was determined using a modified Helm's test with an additional gentle agitation step as described in the materials and methods. Symbols with brackets represent comparison between light and dark conditions per strain, while symbols without brackets represent a comparison to the CEN.PK113-7D as reference. All Opto-FLO strains grown in light showed a significantly higher flocculation coefficients compared to strains grown in darkness ($P > 0.05$, ** $P < 0.01$, **** $P < 0.001$). Additionally, all Opto-FLO strains, including IMK1061, showed a significantly higher flocculation coefficient relative to CEN.PK113-7D ($P > 0.05$, * $P < 0.05$, *** $P < 0.001$). As expected, IMX2897 did not significantly differ between light and dark conditions. The bars for IMX2912, IMX2913, IMX2914 and IMX2915 represent average values of seven separate experiments, while the CEN.PK113-7D, IMK1061 and IMX2897 represent single experiments. The experiments were performed using biological duplicates with the flocculation assays performed in triplicates. All strains grown in darkness showed no significant difference in flocculation coefficient relative to CEN.PK113-7D. Each open triangle represents a datapoint. Error bars represent the standard deviation. Statistical significance was calculated using multiple unpaired two sided t-tests. P-values were corrected for multiple comparisons using the Holm-Šidák method.

that from prior research does not yield flocculation and IMX2897 (*floΔ X-2::OptoQ::GFP* only) also showed a 30% reduction, indicating the effect stems from OptoQ-AMP5 activation rather than flocculin expression. Induction of FLO expression by blue light (465 nm) for two hours produced clear flocculation differences (Figure 5). IMX2912 (*floΔ X-2::OptoQ::FLO1*), IMX2913 (*floΔ X-2::OptoQ::FLO5*), and, to a lesser extent, IMX2915 (*floΔ X-2::OptoQ::FLO10*) sedimented rapidly, with flocculation coefficient above 87%, with Flo1 reaching 94% (Figure 5 and Supplemental videos 1 and 2). IMX2914 (*floΔ X-2::OptoQ::FLO9*) and IMK1061 (*sf1Δ*) reached 67% and only 37%, respectively (Figure 5). IMX2916 (*floΔ X-2::OptoQ::FLO11*) did not show any flocculation in line with prior studies (Lambrechts et al. 1996, Guo et al. 2000). Under darkness, flocculation coefficients ranged from 4% to 16%, although slight leakiness was detected. Microscopy confirmed as well notable differences in floc structure amongst the different FLO-expressing strains (Figure 6). IMX2912 (*floΔ X-2::OptoQ::FLO1*) formed dense flocs of varying sizes, with some reaching consider-

able dimensions (interquartile range (IQR) of 693–9363 μm^2) (Figure 6A), IMX2913 (*floΔ X-2::OptoQ::FLO5*) formed larger, but less compact flocs (IQR of 1598–15 961 μm^2), while IMX2914 (*floΔ X-2::OptoQ::FLO9*), and IMX2915 (*floΔ X-2::OptoQ::FLO10*) produced smaller ones with an IQR of 136 to 545 and 652 μm^2 for IMX2914 (*floΔ X-2::OptoQ::FLO9*), and (*floΔ X-2::OptoQ::FLO10*), respectively (Figure 6). Despite IMK1061 (*sf1Δ*) flocs being larger, they were less compact and had lower flocculation coefficients. IMX2916 (*floΔ X-2::OptoQ::FLO11*) did not form detectable flocs.

Sugar inhibition phenotypes of *S. cerevisiae* flocculins

To investigate how the fermentable sugars in wort affect the flocculation phenotype of specific flocculins, flocculation assay was modified to include wort sugars (Van Mulders et al. 2009). The inhibitory effects of different fermentable sugars on the flocculation activities of Flo1, Flo5, Flo9, and Flo10 were analysed (Figure 7). On

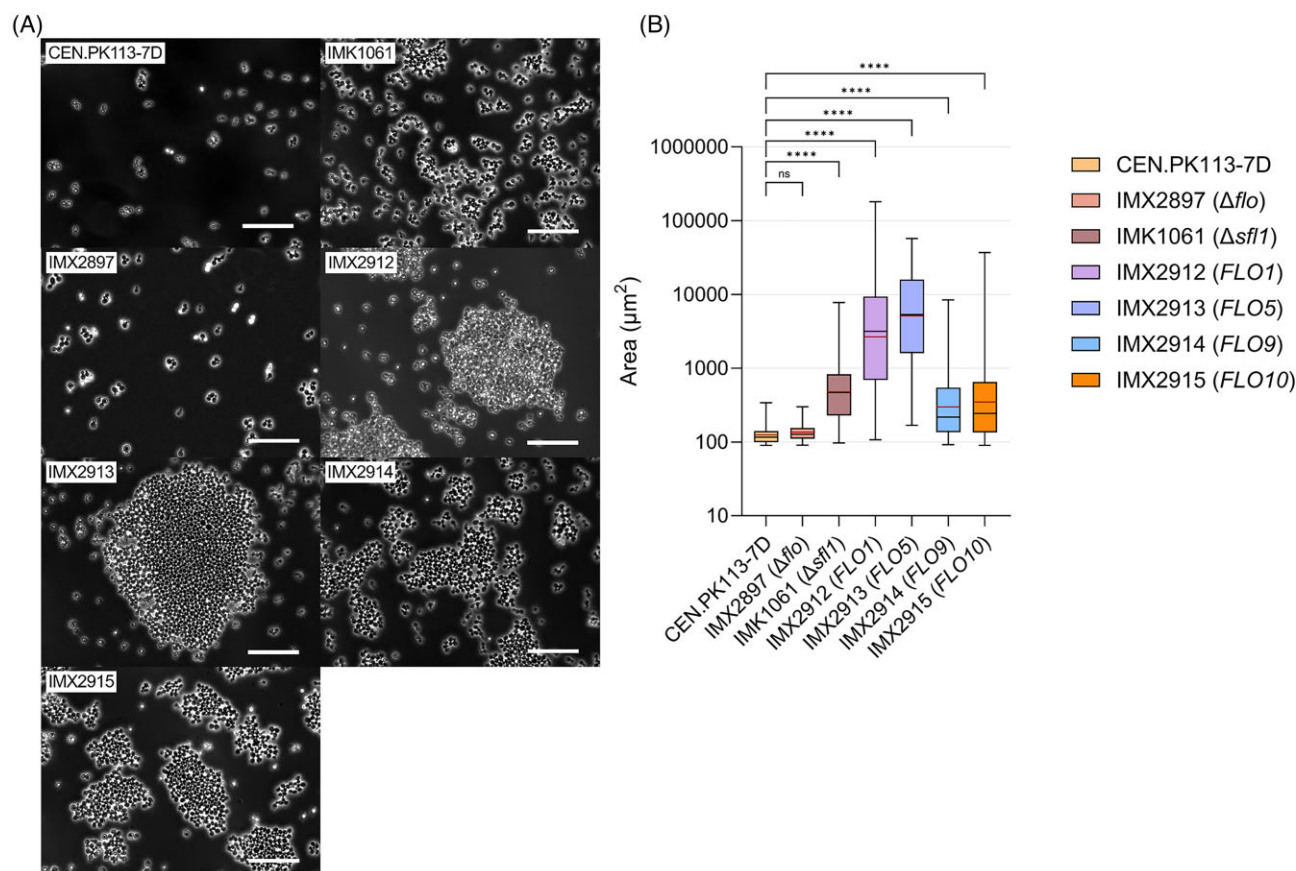


Figure 6. (A) Microscopy of *FLO* expressing strains imaged at 400x magnification. *FLO1* (IMX2912) induced compact floc formation, while *FLO5* (IMX2913) expression resulted in larger, less compact flocs. *FLO9* (IMX2914), *FLO10* (IMX2915) and the *SFL1* deletion (IMK1061) induced small to medium sized floc formation. The *FLO*-null strain (IMX2897) and CEN.PK113-7D exhibited limited to no aggregation. The white bar represents 50 μm. **(B)** Floc size distribution based on the area of cell aggregates imaged at 200x magnification. All flocculating strains showed a significant increase in particle size compared to CEN.PK113-7D (**** $p < 0.0001$). IMX2912 and IMX2913 showed the largest particles, while IMK1061, IMX2914 and IMX2915 showing a similar, smaller distribution of particle sizes. Additionally, IMX2912 and IMX2913 produced flocs much larger than was possible to measure using conventional microscopy, meaning the data is skewed to a lower size relative to actual conditions. All particles smaller than 90 μm² were filtered out to remove aggregates smaller than two aggregated budding cells. Statistical significance was calculated using a Lognormal One-way ANOVA test. Each box represents the 25th to 75th percentile, with the whiskers indicating the minimum and maximum values. The black line represents the median, while the red line represents the geometric mean of the samples. The amount of cell aggregates analyzed per strain ranged from 59 to 182.

the top of mannose, glucose, maltose, and sucrose inhibitions previously investigated, our study included maltotriose, fructose and a mix of all sugars to complete the set of carbohydrates found in wort.

FLO1 (IMX2912) and *FLO5* (IMX2913) displayed a mannose-sensitive *Flo1* phenotype (Stratford and Assinder 1991). Remarkably, inhibition of *Flo5*-induced flocculation was only partially inhibited remaining > 66% even at high mannose concentration, contrasting with previous observations (Govender et al. 2008, Van Mulders et al. 2009, Veelders et al. 2010). Conversely, *Flo9* and *Flo10* were sensitive to a broader sugar spectrum, with *Flo9* strongly inhibited by sucrose and fructose (Figure 7). *Flo1* and *Flo5* resisted maltotriose inhibition, while *Flo9* and *Flo10* were inhibited. Notably, IMX2912 (*floΔ* X-2::OptoQ::FLO1) and IMX2913 (*floΔ* X-2::OptoQ::FLO5) flocculated immediately upon maltotriose addition, reversed by EDTA, suggesting metal contamination of the maltotriose solution (Figure S5). The strains IMX2914 (*floΔ* X-2::OptoQ::FLO9) and IMX2915 (*floΔ* X-2::OptoQ::FLO10) remained in suspension showing complete inhibition. A sugar mix representative of wort comprising 2.5% glucose, 28.0% maltose, 42.0% maltotriose, and 26.4% higher saccharides (w/w) inhibited *Flo1*, *Flo9*, and *Flo10*, but had limited effect on *Flo5*.

Expression of *FLO* genes alters cell surface hydrophobicity

Flocculating strains generally exhibit increased cell surface hydrophobicity (Govender et al. 2008; Purevdorj-Gage et al. 2007; Teixeira et al. 1995; Holle et al. 2012; Van Mulders et al. 2009). Using a dodecane partitioning assay (Figure 8), the positive control strain IMK1061 (*sfl1Δ*) that constitutively expresses all CEN.PK-derived *FLO* genes showed consistently high hydrophobicity independently of the presence of blue light. The *FLO* expressing strains IMX2912-2915 showed higher hydrophobicity under blue light than in darkness. Of the four *FLO* gene expressing strains, IMX2915 (*floΔ* X-2::OptoQ::FLO10) gave the highest value ($73.45 \pm 8.3\%$) followed by IMX2912 (*floΔ* X-2::OptoQ::FLO1) ($68.0 \pm 1.9\%$), while IMX2913 (*floΔ* X-2::OptoQ::FLO5) and IMX2914 (*floΔ* X-2::OptoQ::FLO9) showed lower surface hydrophobicity ($47.7 \pm 0.0\%$ and $50.2 \pm 3.4\%$ respectively). Although IMX2916 (*floΔ* X-2::OptoQ::FLO11) does not flocculate, the expression of *FLO11* and its subsequent display at the cell surface alters cell surface hydrophobicity to a level comparable to that observed in strains expressing *FLO1* and *FLO10*. (Figure 8). Thus, yeast cells rapidly adapted their surface after only 2 hours of *FLO* gene expression.

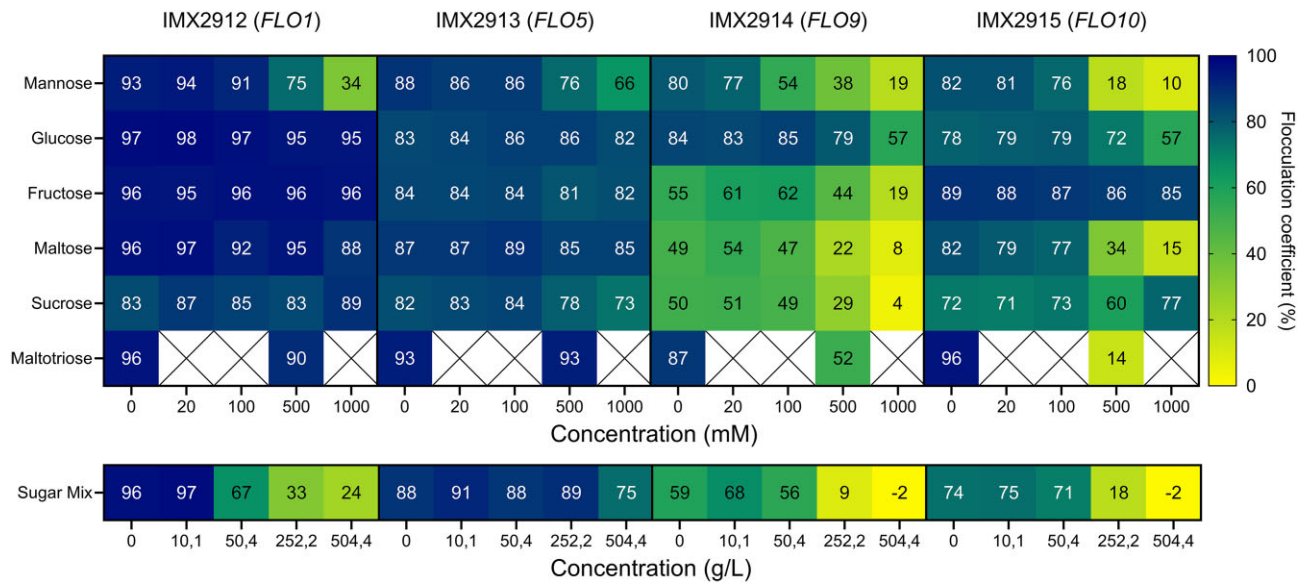


Figure 7. Sugar inhibition profiles of IMX2912 (*floΔ X-2::OptoQ::FLO1*), IMX2913 (*floΔ X-2::OptoQ::FLO5*), IMX2914 (*floΔ X-2::OptoQ::FLO9*) and IMX2915 (*floΔ X-2::OptoQ::FLO10*). Strains were subjected to a modified Helm’s test using flocculation buffer with increasing sugar concentrations (0, 20, 100, 500 and 1000 mM) to determine the sensitivity of each flocculin to the various sugars tested. Additionally, sensitivity to a sugar mix used as an adjunct to wort was determined (2.5% glucose, 28.0% maltose, 42.0% maltotriose, and 26.4% higher saccharides (w/w)).

Discussion

Yeasts contain a diverse array of *FLO* genes with roles that vary depending on physiological, social and environmental context. Their complex regulation and phenotypic diversity pose significant challenges for functional studies. To address this, we developed a *FLO*-null platform strain enabling systematic analysis of *FLO* gene functions. Such null-strain platforms have advanced gene families studies e.g. the *HXT*-null strain (Wieczorke et al. 1999, Wijsman et al. 2019), which has been instrumental in characterizing both native and heterologous sugar transporters, including human glucose transporters (Wieczorke et al. 1999, Solis-Escalante et al. 2015, Tripp et al. 2017, Nijland and Driessen 2020, Schmidl et al. 2021) and *ALD*-null strain devoid of aldehyde dehydrogenase pivotal for acetate metabolism and utilisation of ethanol as carbon source for biotechnological processes (Saint-Prix et al. 2004, Kozak et al. 2016).

Here, we used optogenetics with the *FLO*-null strain to characterise *FLO* gene function. Optogenetics provide precise temporal control mimicking dynamic *FLO* gene induction while bypassing native regulation. Within two hours of blue light induction diverse flocculation phenotypes emerged. Flo1 and Flo5 produced the strongest aggregation with Flo1 yielding denser flocs and Flo5 forming larger aggregates consistent with earlier reports (Figures 5 and 7) (Guo et al. 2000, Fichtner et al. 2007, Govender et al. 2008, Van Mulders et al. 2009). These structural differences may influence stress resistance and mass transfer during fermentation (Ge et al. 2006). We propose that floc size and density also shape yeast social behaviour. Flo1 may preferentially mediate self-self-interactions via the green beard effect (Smukalla et al. 2008), whereas Flo5 may allow incorporation of non-self-cells. Yet, Rossouw et al. (2015) found Flo5 reduced mixed-species floc formation relative to Flo1, highlighting strain—dependent variation.

By contrast, *FLO9*’s role remains unclear. Overexpression in *S. cerevisiae* BY4700 strain and in *Kluyveromyces marxianus* induced strong flocculation (Nonklang et al. 2009), but IMX2914 (*floΔ X-2::OptoQ::FLO9*) showed weaker, less stable aggregation, dispers-

ing after 30 s of vortexing (Van Mulders et al. 2009). Differences likely stems from fewer type-1 repeats in CEN.PK Flo9 versus S288c and BY4700 (Tables 3 and 4). These results underscore how repeat variation or background-specific sequence changes strongly affect flocculation.

CEN.PK normally lacks flocculation despite an intact *FLO8*, unlike S288C that carries a premature stop codon and where *FLO8* restoration confers strong aggregation (Liu et al. 1996, Bester et al. 2006, Fichtner et al. 2007). In CEN.PK strains, *SFL1* deletion produced only weak flocculation, suggesting reduced *FLO* expression and weaker adhesion. Transcriptional analysis of *FLO* genes under *SFL1* deletion and/or *FLO8* overexpression could clarify their contributions in transcriptional regulation.

For brewing purposes, understanding sugar effects is essential. Sugar inhibition assays revealed distinct inhibition profiles across the *FLO*-expressing strains. IMX2912 (*floΔ X-2::OptoQ::FLO1*) displayed a Flo1-type flocculation phenotype, characterised by sensitivity to mannose, while IMX2914 (*floΔ X-2::OptoQ::FLO9*) and IMX2915 (*floΔ X-2::OptoQ::FLO10*) showed “NewFlo-type” flocculation phenotype, with IMX2914 (*floΔ X-2::OptoQ::FLO9*) uniquely sensitive to fructose and sucrose, previously unreported for *FLO* genes though observed in *Saccharomyces uvarum* wine strains (Amri et al. 1979, Suzzi et al. 1992, Berthels et al. 2004, Guillaume et al. 2007). Flo9 and Flo10 also displayed sensitivity to maltotriose, another novel observation. Surprisingly, IMX2912 (*floΔ X-2::OptoQ::FLO1*) and IMX2913 (*floΔ X-2::OptoQ::FLO5*) flocculated instantly after flocculation buffer addition to deflocculated cells without Ca^{2+} (Figure S5), suggesting that the maltotriose used may have been contaminated with Ca^{2+} or other metal ions that might induce flocculation. Nevertheless, neither strain displayed inhibition of flocculation by maltotriose itself. Little is currently known about the metal ion specificity of individual Flo proteins and this was not observed with the sugar mix, containing approximately 42% maltotriose. Further investigation into the metal ion specificity of Flo proteins is therefore warranted.

Interestingly, IMX2913 (*floΔ X-2::OptoQ::FLO5*) showed minimal sugar sensitivity, despite prior reports of strong inhibition by man-

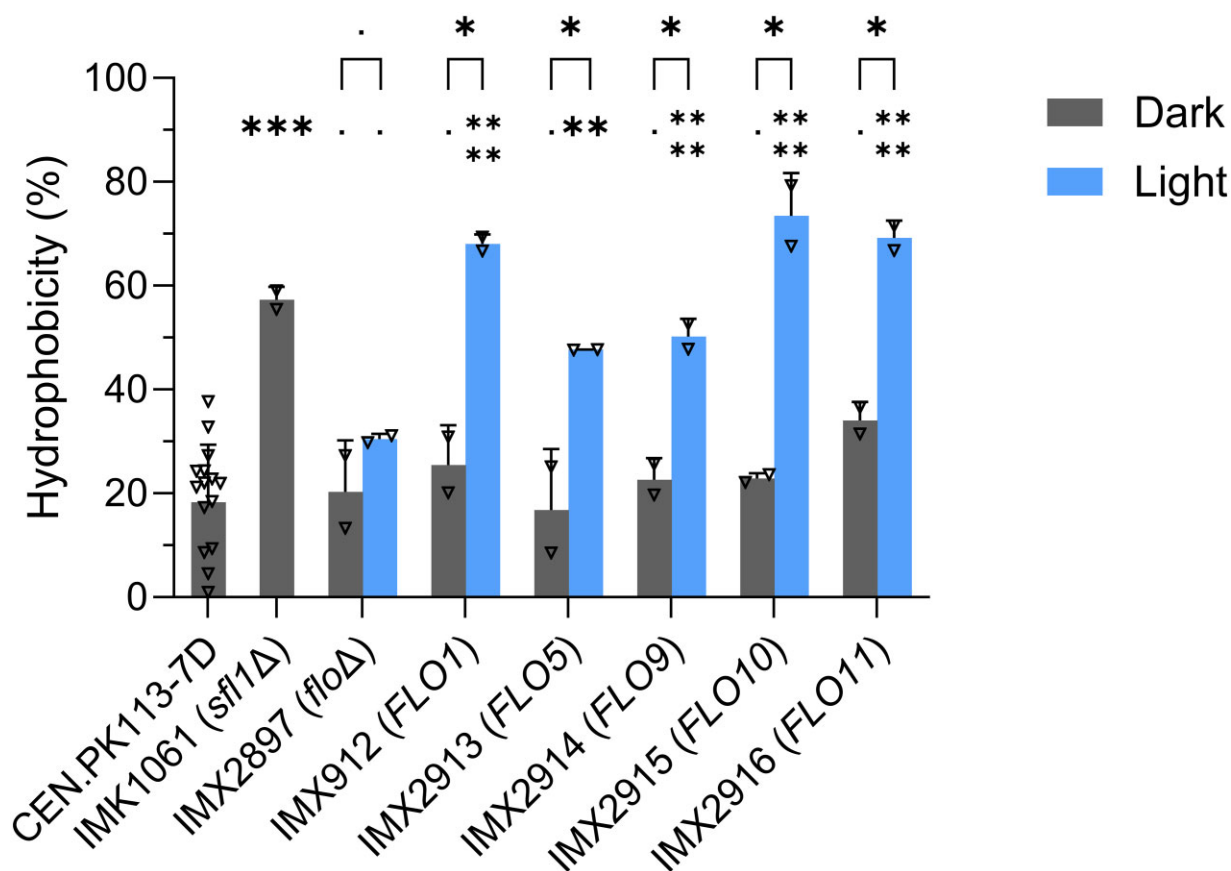


Figure 8. Determination of cell surface hydrophobicity of CEN.PK113-7D, IMK1061 (*sf11Δ*), IMX2897 (*floΔ X-2::OptoQ::AMP5*), IMX2912 (*floΔ X-2::OptoQ::FLO1*), IMX2913 (*floΔ X-2::OptoQ::FLO5*), IMX2914 (*floΔ X-2::OptoQ::FLO9*), IMX2915 (*floΔ X-2::OptoQ::FLO10*) and IMX2916 (*floΔ X-2::OptoQ::FLO11*) grown under light and dark conditions. The hydrophobicity percentage is calculated by the ratio of cells partitioning between an aqueous phase and a dodecane organic phase. All bars represent average values of experiments using biological duplicates and measured in technical duplicates. The CEN.PK113-7D bar represents the average of all control measurements done per experiment. Symbols with brackets represent comparison between light and dark conditions per strain, while symbols without brackets represent a comparison to the CEN.PK113-7D as reference. IMX2912, IMX2913, IMX2914, IMX2915 and IMX2916 exhibited a significant increase in hydrophobicity under light conditions relative to dark conditions (* $P < 0.05$). Additionally, all Opto-FLO strains and IMK1061 showed a significantly higher hydrophobicity relative to CEN.PK113-7D (* $P < 0.05$, ** $P < 0.01$, *** $P < 0.0001$). IMX2897 did not significantly differ between light and dark conditions. All strains grown in darkness showed no significant difference in hydrophobicity relative to CEN.PK113-7D. Each open triangle represents a datapoint. Error bars represent the standard deviation. Statistical significance was calculated using multiple unpaired two sided t-tests. P-values were corrected for multiple comparisons using the Holm-Sidak method.

nose, maltose and sucrose (Bidard et al. 1994, Govender et al. 2008, Van Mulders et al. 2009, Veelders et al. 2010). As *FLO5*_{CEN.PK} is identical to S288C (Table S3), differences may arise from epistatic effects such as altered glycosylation. Indeed, heterologous *FLO10* expression yields background specific phenotypes (Nonklang et al. 2009) and post translational modifications like phosphorylation may further modulate activity (Leutert et al. 2023). A sugar mix consisting of maltotriose, maltose, glucose and higher weight dextrans (e.g. maltotetraose and maltopentose), strongly inhibited flocculation in most strains but only modestly affected IMX2913 (*floΔ X-2::OptoQ::FLO5*). That dextrans inhibited IMX2912 (*floΔ X-2::OptoQ::FLO1*) flocculation would suggest that not only single sugar, but also interaction and synergistic effect between saccharides may exacerbate the phenotype. These results could also imply that dextrans which have been reported to inhibit flocculation (Stratford and Assinder 1991), specifically target Flo1. The impact of flocculins on cell surface hydrophobicity is decoupled from their flocculation properties. As demonstrated with *FLO11*, its expression and surface display are sufficient to alter hydrophobicity, although this does not induce flocculation. This effect is primar-

ily attributed to mannan glycosylation. Similarly to sugar inhibition, even minor differences in post-translational modifications such as glycosylation, can significantly influence the hydrophobic properties of flocculins.

In a broader context, adhesins play critical roles in the virulence of numerous pathogenic fungi, for example: Als (Agglutinin-Like Sequence) and Epa (Epithelial Adhesin) families in *Candida* species (Dranginis et al. 2007), Cfl1 (Cell Flocculin 1) in *Cryptococcus neoformans* (Wang et al. 2012) and RodA hydrophobins in *Aspergillus fumigatus* (Thau et al. 1994). *Saccharomyces* species could also be considered as emerging pathogens for people who present immune system deficiencies (Pérez-Torrado and Querol 2016). The *FLO*-null platform with the optogenetic control thus provides a versatile and scalable system for dissecting adhesion phenotypes and intercellular interactions across diverse Flo proteins. By allowing precise spatiotemporal control of adhesin expression in a uniform genetic background, this system will enable systematic structure-to-function analyses of adhesins and facilitate engineering of tailored adhesion properties for industrial or even biomedical purposes.

Conclusion

We successfully constructed a *Saccharomyces cerevisiae* CEN.PK113-7D strain lacking all known *FLO* genes and demonstrated its utility as a platform for controlled functional characterization. Using an optogenetic network circuit to precisely regulate *FLO1*, *FLO5*, *FLO9*, and *FLO10*, we observed a diverse range of flocculation phenotypes including differences in floc size distributions, sedimentation rates, sugar sensitivity and cell surface hydrophobicity. These results highlight the versatility of this optogenetic *FLO*-null system for advancing our understanding of flocculation and open new avenues for the rational design of yeast strains tailored for industrial fermentation processes that require tuneable and stable flocculation.

Author contributions

J.M.G.D., N.X.B. and D.G.L.I. designed the experiments. D.G.L.I., N.X.B. and D.C.C. performed the characterization of the OptoQ-AMP5 and qPCR experiments. D.G.L.I. conducted the Flo protein sequence analysis. D.G.L.I., C.W., L.T. and J.K. investigated the characterization of the *FLO* genes using the *FLO*-null strain platform. D.G.L. and J.M.G.D. supervised the study. D.G.L.I. and J.M.G.D. wrote the manuscript. All authors read and approved the final manuscript.

Acknowledgements

We would like to thank Philip de Groot for aiding in the sampling of cultures for the evaluation of the inducibility of the OptoQ-AMP5 optogenetic circuit. We are thankful to Prof. J.T. Pronk (Delft University of Technology), Dr. V.M. Boer and Mr T. Elink-Schuurman for their support during this project.

Supplementary data

Supplementary data are available at [FEMSyr Journal](https://femsyr.journalonline.com) online.

Conflict of interest : The authors have no conflict of interest to declare.

Funding

This work was performed within the Top consortia for Knowledge and Innovation (TKIs) AgriFood which was granted a PPP allowance from the Ministry of Economic Affairs and Climate Policy (Project Habitats #PPPS1701).

Data availability

Data underlying this study are available at the the 4TU research repository (<https://data.4tu.nl/>) under the following DOI: <https://doi.org/10.4121/62ba86ed-f06f-4a6d-9551-02ba06ee3e52>.

References

Amri MA, Bonaly R, Duteurtre B et al. Growth and flocculation of two *Saccharomyces uvarum* strains. *Eur J Appl Microbiol Biotechnol* 1979;**7**:227–34. <https://doi.org/10.1007/BF00498016>.

Ansanay Galeote V, Alexandre H, Bach B et al. Sfl1p acts as an activator of the HSP30 gene in *Saccharomyces cerevisiae*. *Curr Genet* 2007;**52**:55–63. <https://doi.org/10.1007/s00294-007-0136-z>.

Bernardi B, Kayacan Y, Wendland J. Expansion of a Telomeric *FLO*/ALS-Like Sequence Gene Family in *Saccharomycopsis fermentans*. *Front Genet* 2018;**9**:536. <https://doi.org/10.3389/fgene.2018.00536>.

Berthels NJ, Cordero Otero RR, Bauer FF et al. Discrepancy in glucose and fructose utilisation during fermentation by *Saccharomyces cerevisiae* wine yeast strains. *FEMS Yeast Res* 2004;**4**:683–9. <https://doi.org/10.1016/j.femsyr.2004.02.005>.

Bester MC, Pretorius IS, Bauer FF. The regulation of *Saccharomyces cerevisiae* *FLO* gene expression and Ca²⁺-dependent flocculation by Flo8p and Mss11p. *Curr Genet* 2006;**49**:375–83. <https://doi.org/10.1007/s00294-006-0068-z>.

Bidard F, Blondin B, Dequin S et al. Cloning and analysis of a *FLO5* flocculation gene from *S. cerevisiae*. *Curr Genet* 1994;**25**:196–201. <https://doi.org/10.1007/BF00357162>.

Blum M, Andreeva A, Florentino LC et al. InterPro: the protein sequence classification resource in 2025. *Nucleic Acids Res* 2024;**53**:D444–56. <https://doi.org/10.1093/nar/gkae1082>.

Bouwknegt J, Wiersma SJ, Ortiz-Merino RA et al. A squalene-hopene cyclase in *Schizosaccharomyces japonicus* represents a eukaryotic adaptation to sterol-limited anaerobic environments. *Proc Natl Acad Sci U S A*. 2021;**118**:e2105225118. <https://doi.org/10.1073/pnas.2105225118>.

Burns JA. Yeast flocculation. *J Inst Brew* 1937;**43**:31–43. <https://doi.org/10.1002/j.2050-0416.1937.tb05711.x>.

Caro LHP, Tettelin H, Vossen JH et al. In silico identification of glycosyl-phosphatidylinositol-anchored plasma-membrane and cell wall proteins of *Saccharomyces cerevisiae*. *Yeast* 1997;**13**:1477–89. [https://doi.org/10.1002/\(SICI\)1097-0061\(199712\)13:15<1477::AID-YEA184>3.0.CO;2-L](https://doi.org/10.1002/(SICI)1097-0061(199712)13:15<1477::AID-YEA184>3.0.CO;2-L).

Conlan RS, Tzamarias D. Sfl1 functions via the corepressor Ssn6-Tup1 and the cAMP-dependent protein kinase Tpk2. *J Mol Biol* 2001;**309**:1007–15. <https://doi.org/10.1006/jmbi.2001.4742>.

D'Hautcourt O, Smart KA. Measurement of brewing yeast flocculation. *J Am Soc Brew Chem* 1999;**57**:123–8. <https://doi.org/10.1094/asbcj-57-0123>.

Deed RC, Fedrizzi B, Gardner RC. *Saccharomyces cerevisiae* *FLO1* gene demonstrates genetic linkage to increased fermentation rate at low temperatures. *G3: genes, genomes. Genetics* 2017;**7**:1039–48. <https://doi.org/10.1534/g3.116.037630>.

Der Vaart JM, te Biesebeke R, Chapman JW et al. The beta-1,6-glucan containing side-chain of cell wall proteins of *Saccharomyces cerevisiae* is bound to the glycan core of the GPI moiety. *FEMS Microbiol Lett* 1996;**145**:401–7. <https://doi.org/10.1111/j.1574-6968.1996.tb08607.x>.

Di Gianvito P, Tesnière C, Suzzi G et al. *FLO5* gene controls flocculation phenotype and adhesive properties in a *Saccharomyces cerevisiae* sparkling wine strain. *Sci Rep* 2017;**7**:1–12. <https://doi.org/10.1038/s41598-017-09990-9>.

Dranginis AM, Rauco JM, Coronado JE et al. A biochemical guide to yeast adhesins: glycoproteins for social and antisocial occasions. *Microbiol Mol Biol Rev* 2007;**71**:282–94. <https://doi.org/10.1128/mmbr.00037-06>.

Entian KD, Kötter P. 25 Yeast genetic strain and plasmid collections. *Methods Microbiol* 2007;**36**:629–66. [https://doi.org/10.1016/S0580-9517\(06\)36025-4](https://doi.org/10.1016/S0580-9517(06)36025-4).

Fichtner L, Schulze F, Braus GH. Differential Flo8p-dependent regulation of *FLO1* and *FLO11* for cell-cell and cell-substrate adherence of *S. cerevisiae* S288C. *Mol Microbiol* 2007;**66**:1276–89. <https://doi.org/10.1111/j.1365-2958.2007.06014.x>.

Gagiano M, Van Dyk D, Bauer FF et al. Msn1p/Mss10p, Mss11p and Muc1p/Flo11p are part of a signal transduction pathway downstream of Mep2p regulating invasive growth and pseudohyphal differentiation in *saccharomyces cerevisiae*. *Mol Micro*

- biol 1999;**31**:103–16. <https://doi.org/10.1046/j.1365-2958.1999.01151.x>.
- Ge XM, Zhang L, Bai FW. Impacts of yeast floc size distributions on their observed rates for substrate uptake and product formation. *Enzyme Microb Technol* 2006;**39**:289–95. <https://doi.org/10.1016/j.enzmictec.2005.10.026>.
- Gietz RD, Woods RA. Transformation of yeast by lithium acetate/single-stranded carrier DNA/polyethylene glycol method. *Methods Enzymol* 2002;**350**:87–96. [https://doi.org/10.1016/S0076-6879\(02\)50957-5](https://doi.org/10.1016/S0076-6879(02)50957-5).
- Goossens K, Willaert R. Flocculation protein structure and cell-cell adhesion mechanism in *Saccharomyces cerevisiae*. *Biotechnol Lett* 2010;**32**:1571–85. <https://doi.org/10.1007/s10529-010-0352-3>.
- Goossens K, Ielasi FS, Nookaew I et al. Molecular mechanism of flocculation self-recognition in yeast and its role in mating and survival. *mBio* 2015;**6**:1–16. <https://doi.org/10.1128/mBio.00427-15>.
- Gorter De Vries AR, Voskamp MA, Van Aalst ACA et al. Laboratory evolution of a *Saccharomyces cerevisiae* × *S. eubayanus* hybrid under simulated lager-brewing conditions. *Front Genet* 2019;**10**. <https://doi.org/10.3389/fgene.2019.00242>.
- Govender P, Domingo JL, Bester MC et al. Controlled expression of the dominant flocculation genes FLO1, FLO5, and FLO11 in *Saccharomyces cerevisiae*. *Appl Environ Microb* 2008;**74**:6041–52. <https://doi.org/10.1128/AEM.00394-08>.
- Grünler A, Walther A, Lämmel J et al. Analysis of flocculins in *Ashbya gossypii* reveals FIG2 regulation by TEC1. *Fung Genet Biol* 2010;**47**:619–28. <https://doi.org/10.1016/j.fgb.2010.04.001>.
- Guillaume C, Delobel P, Sablayrolles JM et al. Molecular basis of fructose utilization by the wine yeast *saccharomyces cerevisiae*: a mutated HXT3 allele enhances fructose fermentation. *Appl Environ Microb* 2007;**73**:2432–9. <https://doi.org/10.1128/AEM.02269-06>.
- Guo B, Styles CA, Feng Q et al. A *Saccharomyces* gene family involved in invasive growth, cell-cell adhesion, and mating. *Proc Natl Acad Sci USA* 2000;**97**:12158–63. <https://doi.org/10.1073/pnas.220420397>.
- Halme A, Bumgarner S, Styles C et al. Genetic and epigenetic regulation of the FLO gene family generates cell-surface variation in yeast. *Cell* 2004;**116**:405–15. [https://doi.org/10.1016/S0092-8674\(04\)00118-7](https://doi.org/10.1016/S0092-8674(04)00118-7).
- He Y, Yin H, Dong J et al. Reduced sensitivity of lager brewing yeast to premature yeast flocculation via adaptive evolution. *Food Microbiol* 2022;**106**:104032. <https://doi.org/10.1016/j.fm.2022.104032>.
- Heid CA, Stevens J, Livak KJ et al. Real time quantitative PCR. *Genome Res* 1996;**6**:986–94. <https://doi.org/10.1101/gr.6.10.986>.
- Holle AV, Machado MD, Soares EV Flocculation in ale brewing strains of *Saccharomyces cerevisiae*: re-evaluation of the role of cell surface charge and hydrophobicity. *Appl Microbiol Biotechnol* 2012;**93**:1221–9. <https://doi.org/10.1007/s00253-011-3502-1>.
- Hottiger T, Fürst P, Pohl G et al. Physiological characterization of the yeast metallothionein (CUP1) promoter, and consequences of overexpressing its transcriptional activator, ACE1. *Yeast* 1994;**10**:283–96. <https://doi.org/10.1002/yea.320100302>.
- Hovland P, Flick J, Johnston M et al. Galactose as a gratuitous inducer of GAL gene expression in yeasts growing on glucose. *Gene* 1989;**83**:57–64. [https://doi.org/10.1016/0378-1119\(89\)90403-4](https://doi.org/10.1016/0378-1119(89)90403-4).
- Jentoft N. Why are proteins O-glycosylated? *Trends Biochem Sci* 1990;**15**:291–4. [https://doi.org/10.1016/0968-0004\(90\)90014-3](https://doi.org/10.1016/0968-0004(90)90014-3).
- Juergens H, Varela JA, Gorter de Vries AR et al. Genome editing in *Kluyveromyces* and *Ogataea* yeasts using a broad-host-range Cas9/gRNA co-expression plasmid. *FEMS Yeast Res* 2018;**18**:foy012. <https://doi.org/10.1093/femsyr/foy012>.
- Keleher CA, Redd MJ, Schultz J et al. Ssn6-Tup1 is a general repressor of transcription in yeast. *Cell* 1992;**68**:709–19. [https://doi.org/10.1016/0092-8674\(92\)90146-4](https://doi.org/10.1016/0092-8674(92)90146-4).
- Kim HY, Lee SB, Kang HS et al. Two distinct domains of Flo8 activator mediates its role in transcriptional activation and the physical interaction with Mss11. *Biochem Biophys Res Commun* 2014;**449**:202–7. <https://doi.org/10.1016/j.bbrc.2014.04.161>.
- Kozak BU, van Rossum HM, Niemeijer MS et al. Replacement of the initial steps of ethanol metabolism in *Saccharomyces cerevisiae* by ATP-independent acetylating acetaldehyde dehydrogenase. *FEMS Yeast Res* 2016;**16**:fow006. <https://doi.org/10.1093/femsyr/fow006>.
- Kuijpers NG, Solis-Escalante D, Bosman L et al. A Versatile, Efficient Strategy for Assembly of Multi-Fragment Expression Vectors in *Saccharomyces Cerevisiae* Using 60 Bp Synthetic Recombination Sequences. 2013. <https://doi.org/10.1186/1475-2859-12-47>.
- Kuyper M, Hartog MM, Toirkens MJ et al. Metabolic engineering of a xylose-isomerase-expressing *Saccharomyces cerevisiae* strain for rapid anaerobic xylose fermentation. *FEMS Yeast Res* 2005;**5**:399–409. <https://doi.org/10.1016/j.femsyr.2004.09.010>.
- Lalwani MA, Zhao EM, Wegner SA et al. The *neurospora crassa* Inducible Q system enables simultaneous optogenetic amplification and inversion in *saccharomyces cerevisiae* for bidirectional control of gene expression. *ACS Synth Biol* 2021;**10**:2060–75. <https://doi.org/10.1021/acssynbio.1c00229>.
- Lambrechts MG, Bauer FF, Marmur J et al. Muc1, a mucin-like protein that is regulated by Mss10, is critical for pseudohyphal differentiation in yeast. *Proc Natl Acad Sci USA* 1996;**93**:8419–24. <https://doi.org/10.1073/pnas.93.16.8419>.
- Leutert M, Barente AS, Fukuda NK et al. The regulatory landscape of the yeast phosphoproteome. *Nat Struct Mol Biol* 2023;**30**:1761–73. <https://doi.org/10.1038/s41594-023-01115-3>.
- Li H. Aligning sequence reads, clone sequences and assembly contigs with BWA-MEM. *arXiv* 2013; **Genomics (q-bio.GN)**:1303.3997. <https://doi.org/10.48550/arXiv.1303.3997>.
- Liu H, Styles CA, Fink GR. *Saccharomyces cerevisiae* S288C has a mutation in FLO8, a gene required for filamentous growth. *Genetics* 1996;**144**:967–78. <https://doi.org/10.1093/genetics/144.3.967>.
- Liu N, Wang D, Wang ZY et al. Genetic basis of flocculation phenotype conversion in *Saccharomyces cerevisiae*. *FEMS Yeast Res* 2007;**7**:1362–70. <https://doi.org/10.1111/j.1567-1364.2007.00294.x>.
- Livak KJ, Schmittgen TD. Analysis of relative gene expression data using real-time quantitative PCR and the 2- $\Delta\Delta$ CT method. *Methods* 2001;**25**:402–8. <https://doi.org/10.1006/meth.2001.1262>.
- Madeira F, Madhusoodanan N, Lee J et al. The EMBL-EBI Job Dispatcher sequence analysis tools framework in 2024. *Nucleic Acids Res* 2024;**52**:W521–5. <https://doi.org/10.1093/nar/gkae241>.
- Mans R, van Rossum HM, Wijsman M et al. CRISPR/Cas9: a molecular swiss army knife for simultaneous introduction of multiple genetic modifications in *Saccharomyces cerevisiae*. *FEMS Yeast Res* 2015;**15**:1–15. <https://doi.org/10.1093/femsyr/fov004>.
- Mans R, Wijsman M, Daran-Lapujade P et al. A protocol for introduction of multiple genetic modifications in *Saccharomyces cerevisiae* using CRISPR/Cas9. *FEMS Yeast Res* 2018;**18**:1–13. <https://doi.org/10.1093/femsyr/foy063>.
- Miki BLA, Poon NH, James AP et al. Possible mechanism for flocculation interactions governed by gene FLO1 in *Saccharomyces cerevisiae*. *J Bacteriol* 1982;**150**:878–89. <https://doi.org/10.1128/jb.150.2.878-889.1982>.
- Mikkelsen MD, Buron LD, Salomonsen B et al. Microbial production of indolylglucosinolate through engineering of a multi-gene pathway in a versatile yeast expression platform. *Metab Eng* 2012;**14**:104–11. <https://doi.org/10.1016/j.jymben.2012.01.006>.

- Nijland JG, Driessen AJM. Engineering of pentose transport in *Saccharomyces cerevisiae* for biotechnological applications. *Front Bioeng Biotechnol* 2020;**7**:464 <https://doi.org/10.3389/fbioe.2019.00464>.
- Nonklang S, Ano A, Babiker MAAB et al. Construction of flocculent *Kluyveromyces marxianus* strains suitable for high-temperature ethanol fermentation. *Biosci Biotechnol Biochem* 2009;**73**:1090–5. <https://doi.org/10.1271/bbb.80853>.
- Pan X, Heitman J. Protein kinase A operates a molecular switch that governs yeast pseudohyphal differentiation. *Mol Cell Biol* 2002;**22**:3981–93. <https://doi.org/10.1128/mcb.22.12.3981-3993.2002>.
- Panteloglou AG, Smart KA, Cook DJ. Malt-induced premature yeast flocculation: current perspectives. *J Ind Microbiol Biotechnol* 2012;**39**:813–22. <https://doi.org/10.1007/s10295-012-1086-0>.
- Pérez-Torradó R, Querol A. Opportunistic strains of *Saccharomyces cerevisiae*: a potential risk sold in food products. *Front Microbiol* 2016;**6**:fmicb.2015.01522 <https://doi.org/10.3389/fmicb.2015.01522>.
- Pronk JT. Auxotrophic yeast strains in fundamental and applied research. *Appl Environ Microb* 2002;**68**:2095–100. <https://doi.org/10.1128/AEM.68.5.2095-2100.2002>.
- Purevdorj-Gage B, Orr ME, Stoodley P et al. The role of FLO11 in *Saccharomyces cerevisiae* biofilm development in a laboratory based flow-cell system. *FEMS Yeast Res* 2007;**7**:372–9. <https://doi.org/10.1111/j.1567-1364.2006.00189.x>.
- Robertson LS, Fink GR. The three yeast A kinases have specific signaling functions in pseudohyphal growth. *Proc Natl Acad Sci USA* 1998;**95**:13783–7. <https://doi.org/10.1073/pnas.95.23.13783>.
- Rosenberg M. Bacterial adherence to hydrocarbons: a useful technique for studying cell surface hydrophobicity. *FEMS Microbiol Lett* 1984;**22**:289–95. <https://doi.org/10.1111/j.1574-6968.1984.tb00743.x>.
- Rossouw D, Bagheri B, Setati ME et al. Co-flocculation of yeast species, a new mechanism to govern population dynamics in microbial ecosystems. *PLoS One* 2015;**10**:1–17. <https://doi.org/10.1371/journal.pone.0136249>.
- Rowlands H, Shaban K, Foster B et al. Histone chaperones and the Rrm3p helicase regulate flocculation in *S. cerevisiae*. *Epigenetics Chromatin* 2019;**12**:56. <https://doi.org/10.1186/s13072-019-0303-8>.
- Saint-Prix F, Bönquist L, Dequin S. Functional analysis of the ALD gene family of *Saccharomyces cerevisiae* during anaerobic growth on glucose: the NADP⁺-dependent Ald6p and Ald5p isoforms play a major role in acetate formation. *Microbiology* 2004;**150**:2209–20. <https://doi.org/10.1099/mic.0.26999-0>.
- Salazar AN, Gorter de Vries AR, van den Broek M et al. Nanopore sequencing enables near-complete de novo assembly of *Saccharomyces cerevisiae* reference strain CEN.PK113-7D. *FEMS Yeast Res* 2017;**17**:fox074. <https://doi.org/10.1093/femsyr/fox074>.
- Sampermans S, Mortier J, Soares EV. Flocculation onset in *Saccharomyces cerevisiae*: the role of nutrients. *J Appl Microbiol* 2005;**98**:525–31. <https://doi.org/10.1111/j.1365-2672.2004.02486.x>.
- Sariki SK, Kumawat R, Singh V et al. Flocculation of *Saccharomyces cerevisiae* is dependent on activation of Slt2 and Rlm1 regulated by the cell wall integrity pathway. *Mol Microbiol* 2019;**112**:1350–69. <https://doi.org/10.1111/mmi.14375>.
- Schmidl S, Tamayo Rojas SA, Iancu CV et al. Functional expression of the Human glucose transporters GLUT2 and GLUT3 in yeast offers novel screening systems for GLUT-targeting drugs. *Front Mol Biosci* 2021;**7**:598419 <https://doi.org/10.3389/fmolb.2020.598419>.
- Sievers F, Higgins DG. Clustal Omega for making accurate alignments of many protein sequences. *Protein Sci* 2018;**27**:135–45. <https://doi.org/10.1002/pro.3290>.
- Singh V, Azad GK, Sariki SK et al. Flocculation in *Saccharomyces cerevisiae* is regulated by RNA/DNA helicase Sen1p. *FEBS Lett* 2015;**589**:3165–74. <https://doi.org/10.1016/j.febslet.2015.09.006>.
- Smukalla S, Caldara M, Pochet N et al. FLO1 Is a variable green beard gene that drives biofilm-like cooperation in budding yeast. *Cell* 2008;**135**:726–37. <https://doi.org/10.1016/j.cell.2008.09.037>.
- Solis-Escalante D, Kuijpers NG, Bongaerts N et al. amdSYM, A new dominant recyclable marker cassette for *Saccharomyces cerevisiae*. *FEMS Yeast Res* 2013;**13**:126–39. <https://doi.org/10.1111/1567-1364.12162>.
- Solis-Escalante D, Kuijpers NG, van der Linden FH et al. Efficient simultaneous excision of multiple selectable marker cassettes using I-SceI-induced double-strand DNA breaks in *Saccharomyces cerevisiae*. *FEMS Yeast Res* 2014;**14**:741–54. <https://doi.org/10.1093/femsyr/fou004>.
- Solis-Escalante D, van den Broek M, Kuijpers NG et al. The genome sequence of the popular hexose-transport-deficient *Saccharomyces cerevisiae* strain EBY.VW4000 reveals LoxP/cre-induced translocations and gene loss. *FEMS Yeast Res* 2015;**15**:126–39. <https://doi.org/10.1111/1567-1364.12024>.
- Stewart GG. *Saccharomyces* species in the production of beer. *Beverages* 2016;**2**:34. <https://doi.org/10.3390/beverages2040034>.
- Stewart GG. Yeast flocculation—Sedimentation and flotation. *Fermentation* 2018;**4**:28. <https://doi.org/10.3390/fermentation4020028>.
- Stratford M, Assinder S. Yeast flocculation: flo1 and NewFlo phenotypes and receptor structure. *Yeast* 1991;**7**:559–74. <https://doi.org/10.1002/yea.320070604>.
- Stratford M. Genetic aspects of yeast flocculation: in role of FLO genes in the flocculation of *cerevisiae*. *Colloids Surf B Biointerfaces* 1994;**2**:151–8. [https://doi.org/10.1016/0927-7765\(94\)80029-4](https://doi.org/10.1016/0927-7765(94)80029-4).
- Stratford M. Induction of flocculation in brewing yeasts by change in pH value. *FEMS Microbiol Lett* 1996;**136**:13–18. [https://doi.org/10.1016/0378-1097\(95\)00456-4](https://doi.org/10.1016/0378-1097(95)00456-4).
- Straver MH, Traas VM, Smit G et al. Isolation and partial purification of mannose-specific agglutinin from brewer's yeast involved in flocculation. *Yeast* 1994;**10**:1183–93. <https://doi.org/10.1002/yea.320100906>.
- Suzzi G, Romano P, Benevelli M. The flocculation of wine yeasts: biochemical and morphological characteristics in *zygosaccharomyces*—Flocculation in *zygosaccharomyces*. *Antonie Van Leeuwenhoek* 1992;**61**:317–22. <https://doi.org/10.1007/BF00713939>.
- Tai SL, Boer VM, Daran-Lapujade P., et al. Two-dimensional transcriptome analysis in chemostat cultures. Combinatorial effects of oxygen availability and macronutrient limitation in *Saccharomyces cerevisiae*. *J Biol Chem* 2005;**280**:437–47. <https://doi.org/10.1074/jbc.M410573200>.
- Teixeira JA, Oliveira R, Azeredo J et al. Cell wall surface properties and flocculence of a *Kluyveromyces marxianus* strain. *Colloids Surf B Biointerfaces* 1995;**5**:197–203. [https://doi.org/10.1016/0927-7765\(95\)01227-A](https://doi.org/10.1016/0927-7765(95)01227-A).
- Teste MA, Duquenne M, François JM et al. Validation of reference genes for quantitative expression analysis by real-time RT-PCR in *Saccharomyces cerevisiae*. *BMC Mol Biol* 2009;**10**:99. <https://doi.org/10.1186/1471-2199-10-99>.
- Teunissen AW, van den Berg JA, Steensma HY. Physical localization of the flocculation gene FLO1 on chromosome I of *Saccharomyces cerevisiae*. *Yeast* 1993;**9**:1–10. <https://doi.org/10.1002/yea.320090102>.

- Thau N, Monod M, Crestani B et al. rodletless mutants of *Aspergillus fumigatus*. *Infect Immun* 1994;**62**:4380–8. <https://doi.org/10.1128/iai.62.10.4380-4388.1994>.
- Theunissen A, Steensma HY. Review: the dominant Flocculation genes of *saccharomyces cerevisiae* constitute a new subtelomeric gene family. *Yeast* 1995;**11**:1001–13. <https://doi.org/10.1002/yea.320111102>.
- Tofalo R, Perpetuini G, Di Gianvito P et al. Genetic diversity of FLO1 and FLO5 genes in wine flocculent *saccharomyces cerevisiae* strains. *Int J Food Microbiol* 2014;**191**:45–52. <https://doi.org/10.1016/j.ijfoodmicro.2014.08.028>.
- Tripp J, Essl C, Iancu CV et al. Establishing a yeast-based screening system for discovery of human GLUT5 inhibitors and activators. *Sci Rep* 2017;**7**:6197. <https://doi.org/10.1038/s41598-017-06262-4>.
- Vallejo JA, Sánchez-Pérez A, Martínez JP et al. Cell aggregations in yeasts and their applications. *Appl Microbiol Biotechnol* 2013;**97**:2305–18. <https://doi.org/10.1007/s00253-013-4735-5>.
- van den Broek M, Ortiz-Merino RA, Bennis NX et al. Draft genome sequence of the *Saccharomyces cerevisiae* spy Cas9 expressing strain IMX2600, a laboratory and platform strain from the CEN.PK lineage for cell-factory research. *Microbiol Resour Announc* 2023;**13**:e00550–23. <https://doi.org/10.1128/mra.00550-23>.
- Van Mulders SE, Christianen E, Saerens SMG et al. Phenotypic diversity of Flo protein family-mediated adhesion in *Saccharomyces cerevisiae*. *FEMS Yeast Res* 2009;**9**:178–90. <https://doi.org/10.1111/j.1567-1364.2008.00462.x>.
- Van Mulders SE, Ghequire M, Daenen L et al. Flocculation gene variability in industrial brewer's yeast strains. *Appl Microbiol Biotechnol* 2010;**88**:1321–31. <https://doi.org/10.1007/s00253-010-2843-5>.
- Veelders M, Brückner S, Ott D et al. Structural basis of flocculin-mediated social behavior in yeast. *Proc Natl Acad Sci USA* 2010;**107**:22511–6. <https://doi.org/10.1073/pnas.1013210108>.
- Verduyn C, Postma E, Scheffers WA et al. Effect of benzoic acid on metabolic fluxes in yeasts: a continuous-culture study on the regulation of respiration and alcoholic fermentation. *Yeast* 1992;**8**:501–17. <https://doi.org/10.1002/yea.320080703>.
- Verstrepen KJ, Jansen A, Lewitter F et al. Intragenic tandem repeats generate functional variability. *Nat Genet* 2005;**37**:986–90. <https://doi.org/10.1038/ng1618>.
- Verstrepen KJ, Klis FM. Flocculation, adhesion and biofilm formation in yeasts. *Mol Microbiol* 2006;**60**:5–15. <https://doi.org/10.1111/j.1365-2958.2006.05072.x>.
- Verstrepen KJ, Reynolds TB, Fink GR. Origins of variation in the fungal cell surface. *Nat Rev Micro* 2004;**2**:533–40. <https://doi.org/10.1038/nrmicro927>.
- Wach A, Brachat A, Pohlmann R et al. New heterologous modules for classical or PCR-based gene disruptions in *saccharomyces cerevisiae*. *Yeast* 1994;**10**:1793–808. <https://doi.org/10.1002/yea.320101310>.
- Wang C, Guo Z, Zhan X et al. Structure of the yeast swi/snf complex in a nucleosome free state. *Nat Commun* 2020;**11**:1–8. <https://doi.org/10.1038/s41467-020-17229-x>.
- Wang L, Zhai B, Lin X. The link between morphotype transition and virulence in *Cryptococcus neoformans*. *PLoS Pathog* 2012;**8**:e1002765. <https://doi.org/10.1371/journal.ppat.1002765>.
- Weinhandl K, Winkler M, Glieder A et al. Carbon source dependent promoters in yeasts. *Microb Cell Fact* 2014;**13**:5. <https://doi.org/10.1186/1475-2859-13-5>.
- Wieczorke R, Krampe S, Weierstall T et al. Concurrent knock-out of at least 20 transporter genes is required to block uptake of hexoses in *Saccharomyces cerevisiae*. *FEBS Lett* 1999;**464**:123–8. [https://doi.org/10.1016/S0014-5793\(99\)01698-1](https://doi.org/10.1016/S0014-5793(99)01698-1).
- Wijsman M, Swiat MA, Marques WL et al. A toolkit for rapid CRISPR-SpCas9 assisted construction of hexose-transport-deficient *saccharomyces cerevisiae* strains. *FEMS Yeast Res* 2019;**19**:foyl07. <https://doi.org/10.1093/femsyr/foyl07>.
- Winer J, Kwang C, Jung S et al. Development and validation of real-time quantitative reverse transcriptase-polymerase chain reaction for monitoring gene expression in cardiac myocytes in vitro. *Anal Biochem* 1999;**270**:41–9. <https://doi.org/10.1006/abio.1999.4085>.
- Zhao EM, Zhang Y, Mehl J et al. Optogenetic regulation of engineered cellular metabolism for microbial chemical production. *Nature* 2018;**555**:683–7. <https://doi.org/10.1038/nature26141>.
- Zhou X, Suo J, Liu C et al. Genome comparison of three lager yeasts reveals key genes affecting yeast flocculation during beer fermentation. *Fems Yeast Res* 2021;**29**:1–10. <https://doi.org/10.1093/femsyr/foab031>.